A PROBABILISTIC PROOF OF THURSTON'S CONJECTURE ON CIRCLE PACKINGS

KENNETH STEPHENSON

Contents

The author gratefully asknowledges the support of the National Science Foundation and the Tennessee Science Alliance.

1. Introduction and Main Theorem

1.1. **Opening Remarks.** This paper concerns the approximation of analytic functions using certain configurations of circles called "circle packings", which were first introduced by William Thurston in connection with studies of 3-manifolds. In [30, Chp. 13], he interpreted results of E. M. Andreev [2, 3] concerning hyperbolic polyhedra in terms of circles on the Riemann sphere and found that patterns of circles with prescribed tangency relationships form very rigid structures. This rigidity is reminiscent, at the discrete level, of the rigidity enjoyed by analytic functions *vis-a-vis* infinitesimal circles, and apparently lead Thurston to the conjecture which is the subject of this paper. In a lecture entitled "The Finite Riemann Mapping Theorem," presented at the Bieberbach Conference in 1985, Thurston suggested that the conformal mapping of a bounded simply connected plane domain Ω onto the unit disc $\mathbf{D}$ can be approximated by manipulating hexagonal circle packings lying in Ω.

The Thurston conjecture, as stated, was confirmed by Burt Rodin and Dennis Sullivan [26], with a proof relying heavily on the hexagonal nature of the circle configurations. This hexagonal restriction, however, was not a part of the underlying intuition, and the original purpose of this paper, whose main result was announced in [29], was to prove Thurston's conjecture under much weaker combinatoric hypotheses. As it happens, the topic has progressed and our main result can be proven by what are essentially the Rodin/Sullivan arguments (see [18]); indeed, a yet stronger version has now been proven by Z-X. He and Oded Schramm in [21]. Nonetheless, the proof here, which rests on probabilistic methods involving random walks, provides a unique view into the dynamics of individual circle packings, giving an insight not available with the other approaches to the topic. These dynamics suggest a route to more quantitative results related to harmonic measure, area distortion, and so forth. Moreover, the parameterized families of Markov processes introduced here provide a rich and interesting source of geometrically based processes which may be of independent interest.

We begin with a statement of the main result in a way which avoids the formalities needed later. We then outline our strategy for the proof, stating in particular a Key Lemma whose verification requires the main effort of the paper — it is only in this lemma that the arguments diverge from those used by Rodin and Sullivan in the hexagonal case. We conclude the introductory section by commenting on possible directions for future work, particularly regarding a second aspect of circle packing which has developed since Thurston's talk. This concerns discrete analogues of parts of classical complex function theory. It is quite distinct in character from the approximation theorem which is our objective here; but we require several of its results along the way, so some references to the literature on this developing analogy are given.

1.2. **Statement of the Main Theorem.** Let P denote a finite collection of circles in the plane having mutually disjoint interiors. A geometric 2-complex is formed as follows: Place a vertex at the center of each circle and a euclidean line segment between the centers of any two tangent circles; for each mutually tangent triple of

circles whose interstice contains no other circles of P, place a euclidean triangle using the three centers as vertices. We're interested in circles which are packed together so that this geometric complex triangulates a simply connected closed region; then P is termed a **circle packing** and the geometric complex is called its **carrier**, $\mathbf{carr}\,(P)$. Definitions will necessarily be more formal later, but Figure 1 should convey the basic idea. The set of circle centers from P is denoted $\mathbf{cent}\,(P)$. Circles on the edge of P are **boundary** circles, the others are **interior**. A **flower** consists of a circle and its immediate neighbors, called **petals**. We use the notation $\mathbf{mesh}\,(P)$ in referring to the (euclidean) radius of the largest circle in P.

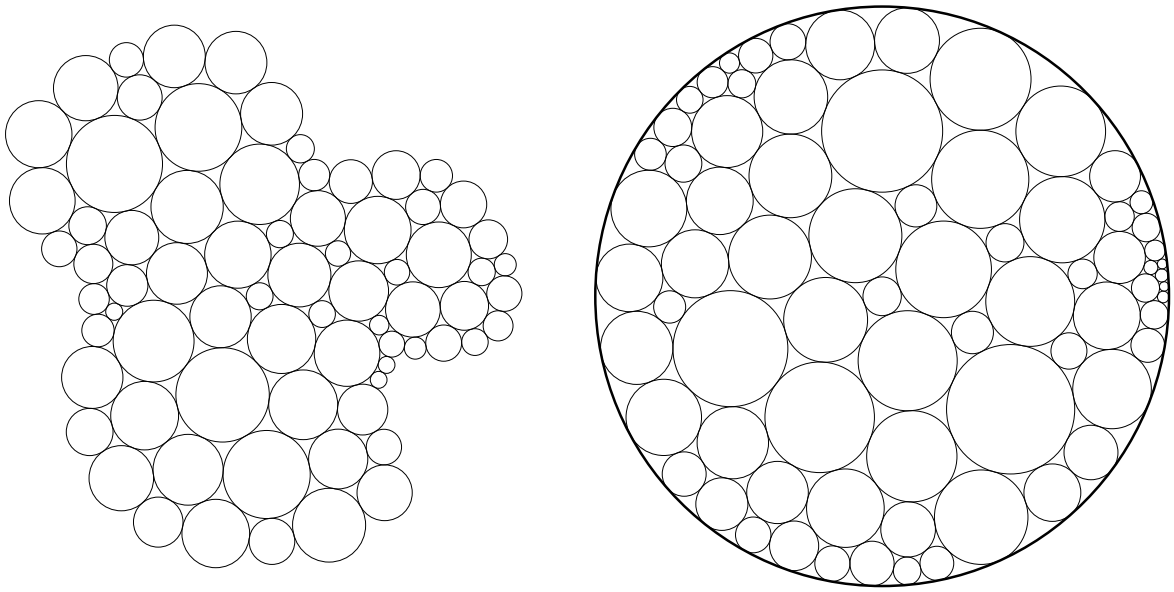

FIGURE 1. Example of a circle packing and it Andreev packing.

To keep track of the combinatorics associated with a circle packing, we introduce the **complex** of P, to be denote by K. This is an abstract oriented simplicial 2-complex equivalent to $\mathrm{carr}\,(P)$; indeed, the latter should be thought of as a simplicial embedding of K in the plane. Boundary circles of P are associated with boundary vertices of K, interior circles with interior vertices, and so forth. The **degree** of a vertex of K is the number of neighboring vertices, and $\mathbf{deg}\,(K)$ is the maximum of the degrees of its vertices. The circle packing P is said to be **hexagonal** if every interior vertex of K has degree 6, and every boundary vertex has degree no more than 6. Two circle packings P_1, P_2 are **combinatorially equivalent** precisely if they have the same abstract complex.

Given a circle packing P, there exists a circle packing $\widetilde{P}$ in the unit disc $\mathbf{D}$ which has the same complex as P but whose boundary circles are internally tangent to the unit circle. (This follows from a result of Koebe [22], but was observed more recently by Thurston [30, Chp. 13].) Being combinatorial equivalent, there is a correspondence

$c \longleftrightarrow \tilde{c}$ between circles of P and $\widetilde{P}$, so that two circles are tangent in P if and only if their counterparts are tangent in $\widetilde{P}$. With normalizations to be specified shortly, $\widetilde{P}$ is unique and we call it the **Andreev packing** for P. The packing on the right in Figure 1 is the Andreev packing associated with the packing on the left.

In the sequel, Ω will be a bounded and simply connected open set in the plane, $z_0, z_1 \in \Omega$ two distinquished points. We will be considering circle packings P lying in Ω and their associated Andreev packings $\widetilde{P}$ in $\mathbf{D}$. It will be an unstated assumption that $z_0, z_1 \in \text{carr}\,(P)$, with z_0 and z_1 in the flowers of distinct interior circles c_0 and c_1. We may modify $\widetilde{P}$ by applying a Möbius transformation of $\mathbf{D}$, if necessary, so that $\tilde{c}_0$ is centered at the origin and $\tilde{c}_1$ is centered on the positive real axis. With these normalizations, we define two functions associated with P:

(1). The **simplicial homeomorphism** $f_P : \text{carr}\,(P) \longrightarrow \text{carr}\,(\widetilde{P})$ is defined by mapping the center of each circle c of P to the center of its counterpart $\tilde{c}$ in $\widetilde{P}$ and then extending *via* euclidean barycentric coordinates to a piecewise affine mapping on the carrier of P (i.e. affine on each face).

(2). The **ratio function** $f_P^{\#} : \text{cent}\,(P) \longrightarrow (0, \infty)$ is defined at the center ζ of a circle c of P by $f_P^{\#}(\zeta) = \tilde{\rho}/\rho$, where ρ is the euclidean radius of c and $\tilde{\rho}$ is the euclidean radius of its counterpart $\tilde{c}$.

It is the simplicial mappings f_P which Thurston proposes as approximations to the conformal mapping of Ω onto $\mathbf{D}$. This is confirmed in our

Main Theorem . *Let $\{P_n\}$ be a sequence of circle packings with carriers lying in Ω and satisfying the following conditions:*

(a). $\text{mesh}\,(P_n) \to 0$ as $n \to \infty$;

(b). the sets $\{\text{carr}\,(P_n)\}$ exhaust Ω;

(c). there exists a constant $1 \leq \mathfrak{C}_r < \infty$ so that for any n, the ratio of the euclidean radii of any two circles in P_n is no greater than $\mathfrak{C}_r$; and

(d). there exists an integer $\mathfrak{d}$ so that for any n, no circle of P_n has more than $\mathfrak{d}$ neighbors.

Let $\{\widetilde{P}_n\}$ denote the associated Andreev packings and let $\{f_n\}$ and $\{f_n^{\#}\}$ be the associated simplicial homeomorphisms and ratio functions, all as defined and normalized above.

Then f_n converges to f uniformly on compact subsets of Ω, where $f : \Omega \longrightarrow \mathbf{D}$ denotes the conformal mapping with $f(z_0) = 0$ and $f(z_1) > 0$. In addition, $f_n^{\#}$ converges uniformly on compact subsets of Ω to $|f'|$.

Conditions (a) and (b) tell us that we have increasingly fine packings which are filling out Ω; in particular, (b) means that they exhaust Ω in the sense of Carathéodory, so every compact subset lies in carr (P_n) for sufficiently large n. Condition (c) is an important condition which enters throughout our proof. It says that the circles comprising each circle packing are comparably sized, and though we put no condition on the constant $\mathfrak{C}_r$ of comparability, it must be independent of n. Condition (d) says that the degree of the complex K_n associated with P_n is bounded by some integer $\mathfrak{d}$, independent of n. The existence of $\mathfrak{d}$ follows easily from condition (c), and has been placed in the statement of the theorem for emphasis — it is the only nonobvious combinatoric restriction on the circle packings P_n. The convergence of the ratio functions $f_n^{\#}$ to $|f'|$ is now quite easy to prove and is included here for completeness; see [14].

In the original conjecture of Thurston [31], the P_n were taken to be hexagonal circle packings, and for each n the circles of P_n were assumed to have identical radii. That case [26, Theorem] follows from our Main Theorem when the constant $\mathfrak{C}_r = 1$. The added flexibility allowed in P_n when $\mathfrak{C}_r > 1$ is reflected both in variable circle size and in the combinatorics of the associated complex, K_n.

1.3. **Summary of the Proof.** Our proof of the Main Theorem is independent of the hexagonal result of Rodin and Sullivan, but it relies on their overall strategy: One first shows *via* elementary geometric facts about flowers of circles that the simplicial mappings f_n have bounded distortion — they are uniformly κ-quasiconformal on their domains carr (P_n) for some $\kappa \geq 1$. By hypothesis, their domains exhaust Ω, and it can be shown using a length-area principle that their ranges exhaust $\mathbf{D}$. As a consequence of quasiconformality, the f_n are equicontinuous on compact subsets of Ω and form a normal family. The additional mapping conditions and normalizations of the f_n ensure that the limit function f of any subsequence is a κ-quasiconformal homeomorphism of Ω onto $\mathbf{D}$ mapping z_0 to the origin and z_1 to the positive axis. This much follows, by-and-large, as in [26], and we will wait on the details until Section 2. Instead, we emphasize the

Key Lemma . *Under the hypotheses of the Main Theorem, given a compact set $E \subset \Omega$ and $\epsilon > 0$, there exists n_0 so that the restriction of f_n to int(E) is $(1+\epsilon)$-quasiconformal for $n > n_0$.*

With this, one concludes that the quasiconformal dilatation of f_n goes to 1 on compacta as $n \to \infty$, hence that the limit function f will be 1-quasiconformal. However, a 1-quasiconformal mapping is conformal. We conclude that f must be the unique conformal mapping of Ω onto $\mathbf{D}$ as claimed in the Main Theorem. The proof of Thurston's conjecture will pivot, then, on the proof of the Key Lemma.

1.4. **Strategy for the Key Lemma.** The main effort of the paper goes into a proof of the Key Lemma. One must show that for large n a triangle T deep within carr (P_n) is not greatly distorted by the mapping f_n.

In the original hexagonal argument of [26] and its extension in [18], verification depends squarely on a theorem of Sullivan regarding the uniqueness of infinite circle packings of the plane. Briefly, their arguments prove that portions of the packings P_n and $\widetilde{P}_n$ behave, for large n, as though they were taken from a single infinite packing. In particular, the ratios of the radii of the circles associated with the triangle T in $\text{carr}\,(P_n)$ will be approximately the same as for the corresponding triangle $\widetilde{T}$ in $\text{carr}\,(\widetilde{P}_n)$, implying that the distortion of f_n on T will be small.

Our proof of the Key Lemma concentrates on the angles of T. If one shows that an angle of T approximates the corresponding angle of $\widetilde{T}$, then again the distortion of f_n on T will be small and the Key Lemma follows. This is the principal theme of the paper: working in hyperbolic geometry, we carry out a thorough study of an individual circle packing P and the dynamics associated with changes in its radii. As indicated, we want to compare a particular angle in some face of $\text{carr}\,(P)$ to the corresponding angle in $\text{carr}\,(\widetilde{P})$. We accomplish this by first developing a differentiable path of parameterized circle packings which starts with P and ends with $\widetilde{P}$; we then estimate the differential of the designated angle along the way. It turns out that infinitesimal radius changes in boundary circles as we move along this path have a rippling effect on the radii of interior circles which works its way through the circle configuration much like electricity moves through an electrical circuit. We are able to model the dynamics at each infinitesimal stage as a Markov process, or random walk. Based on this process we are able to establish a local Harnack inequality, allowing estimates on the differential of the particular angle being watched.

With the details of the proof being rather involved, the author feels that a fuller discussion of the underlying intuition is important — particularly because these ideas may be useful in further studies of circle packings. Therefore, Section 3 provides a more detailed preview of the proof, aided by computer-generated illustrations intended to convey the essential geometric insight. The proof itself requires the succeeding six sections. The paper ends with Section 11, where a fuller discussion of the electrical analogy is possible — it seems like an intuitively appealing and powerful model.

In [18], Z-X. He and Rodin reprove our Main Theorem using the methods of [26] and also prove a stengthened version, removing hypothesis (c), using techniques of [17]. The former method relies finally on the Sullivan uniqueness result for circle packings of the plane, which was proven initially *via* Mostow rigidity, though it now follows from Schramm [27]. The paper of He and Schramm [21] removes both hypotheses (c) and (d) and, through the use of fixed-point index arguments, removes the quasiconformal mapping arguments. It also obtains information on convergence of both first and second derivatives.

The proof here is quite different in character from these other approaches since it is based on an analysis of the dynamics of individual circle packings — an analysis intimately connected to their specific combinatorics. This puts in place machinery for studying various and sundry aspects of circle packing. The proof of the Main

Theorem rests on estimates of certain "escape" probabilities which, *via* diagonalization, we reduce to the celebrated result of Pólya [25] regarding recurrence of the simple random walk on a two-dimensional lattice. If one could improve the analysis of these escape probabilities, one should be able to remove hypotheses (c) and (d) and establish the stronger version due to He/Schramm *via* these same probabilistic methods.

1.5. **Closing Comments.** Circle packing, though a relatively new topic, has generated considerable interest among analysts, topologists, geometers, combinatorists, and others. Representative papers are [1], [5], [8], [9], [10], [16], [12], [19], and [24]. For connections with probability theory, see [7], [20], and [13]. For an introduction to the experimental side with computer software, see [15].

In regard to complex analysis, two lines of inquiry have emerged: One pursues the theme of Thurston's conjecture, using sequences of circle packing maps $f_n : \widetilde{P}_n \to P_n$ in the approximation of classical analytic functions. The other focuses on individual circle packing maps as discrete analogues of analytic functions — their geometric behavior is remarkably faithful to that displayed by their classical counterparts. It is not surprising that these viewpoints are mutually supportive. But a reader intent on the approximation goal should not overlook the real intuition behind this paper, which resides with the analogies — the discrete Schwarz-Pick lemma, the discrete Dirichlet problem, discrete harmonic functions, discrete derivatives. (Branch points have not been needed here, but they too can be defined in an entirely natural way.) These notions appear to the author to provide the fundamental building blocks for a discrete analytic function theory which maintains geometric integrity. The very fact of the Main Theorem certainly suggests that the analogies are far more than superficial parallels. In this same vein, the random walks we use here clearly suggest discrete versions of Brownian motion; indeed, they would represent "killed" processes in which the travelers die in proportion to hyperbolic area. Perhaps the numerous and well known connections among Brownian motion, potential theory, harmonic measure, and analytic function theory can be made available now in this discrete setting.

In regard to other issues, there are two which often arise in discussions of circle packings: (1) **Numerical Conformal Mapping:** It seems unlikely that circle packing methods will compete with traditional methods in numerical conformal mapping in the immediate future, though they might have advantanges in special situations (e.g., multiply-connected regions) or on certain machine architectures. However, the ability to manipulate circle packings could be useful in grid generation, the embedding of graphs, or approximation of discrete Laplace operators. (2) **Sphere Packing:** It is natural to enquire about higher dimensions. However, it seems that little of the topic carries over; as is the case with conformal mappings, sphere packings seem to be extremely rigid in dimensions greater than two. If one injects some added flexibility by considering packings of overlapping spheres or ellipsoids, it is conceivable that the

notion of identifying and studying some conserved geometric quantities, perhaps *via* probabilistic methods, could be of use.

Finally, we mention that the Markov processes defined and used in this paper should be of independent interest to probabilists. There is a process associated with each circle packing for a given complex K, and though we work with these processes only one at a time here, the existence of this vast, coherent family of processes is certainly intriguing — particularly since they have a definite geometric content relating to the movement of hyperbolic curvature. The smooth transition of circle packings from P to $\widetilde{P}$, for example, is paralleled by a "self-modifying" evolution of the associated processes. There are many questions here which deserves closer investigation; the answers may have probablistic proofs and circle packing consequences or *vice verse*.

The author would like to express his appreciation for interesting conversations on various parts of the material presented here with Alan Beardon, Peter Doyle, Keith Carne, Martin Barlow, and Jan Rosinski.

2. Proof Modulo the Key Lemma

2.1. **Introduction.** Here we prove the convergence $f_n \to f$ of the Main Theorem under the assumption, at the appropriate point, that the Key Lemma holds. Our development follows precisely the strategy originated by Rodin and Sullivan for the hexagonal case, and is fairly self-contained, including proofs of the Rodin/Sullivan "ring" and "length-area" lemmas. The notations introduced here will be useful throughout the paper, although we will need to augment them considerably later.

2.2. **Notation.** In the sequel, Ω refers to a fixed bounded, open, simply connected plane region. We may assume without loss of generality that Ω and its closure lie in the open unit disc $\mathbf{D}$, that the distinguished point $z_0 \in \Omega$ is the origin, and that the distinguished point $z_1 \in \Omega$ is a point x lying on the positive real axis.

We will be representing the combinatorics of a circle packing P by an oriented abstract simplicial 2-complex K, with a vertex (0-simplex) for each circle in P, an edge (1-simplex) between the vertices of neighboring (i.e., tangent) circles, and a face (2-simplex) for each triple of mutually tangent circles. The carrier of P, carr (P), which was described earlier, represents an embedding of this abstract complex as a geometric complex in the euclidean plane, while carr $(\widetilde{P})$ is an alternate embedding. We will be working a great deal with these complexes, and it is convenient to note a few restrictions on our configurations which will sidestep some minor pathologies. Thus we will assume in the remainder of the paper that our complexes are equivalent to finite triangulations of closed topological discs. Vertices on the border represent boundary circles and are termed **boundary** vertices, while the others are termed **interior**. Added assumptions are that each boundary vertex shares an edge with at least one interior vertex and that any two interior vertices can be connected by a chain of edges having only interior

vertices as endpoints. Following [5], we will refer to these as **DL-complexes** (for "disc-like") when formality requires it. The configuration of circles and its complex are closely linked, so our discussion will often shift between the two without comment.

The important theorem of Andreev, interpreted in terms of circles by Thurston, implies that every DL-complex is associated with a circle packing: namely, given K, there is a circle packing in the unit disc with complex K whose boundary circles are horocycles (internally tangent to the unit circle); moreover, this circle packing is unique up to automorphisms (Möbius transformations) of the disc. Thus, starting with a circle packing P in Ω, we are lead *via* its underlying complex to what we are calling its **Andreev packing** $\widetilde{P}$. After desired normalizations are made by applying automorphisms to $\widetilde{P}$, the simplicial (orientation-preserving) homeomorphism f mapping $\text{carr}\,(P)$ onto $\text{carr}\,(\widetilde{P})$ may be defined by identifying centers of corresponding circles, extending linearly to the edges, and extending affinely to the faces.

We are considering a sequence P_n of packings in Ω whose carriers exhaust Ω and whose mesh sizes decrease to zero. With these hypotheses, we may assume that for each n, there are disjoint flowers containing 0 and x, say with center circles c_0 and c_x, respectively. If $\tilde{c}_0$ and $\tilde{c}_x$ denote the corresponding circles of the Andreev packing $\widetilde{P}_n$, we assume *via* a normalization that $\tilde{c}_0$ is centered at the origin and $\tilde{c}_x$ is centered on the positive real axis. The corresponding simplicial homeomorphism from $\text{carr}\,(P_n)$ to $\text{carr}\,(\widetilde{P}_n)$ will be denoted by f_n.

2.3. **The Proof.** Our first task will be to prove that the simplicial homeomorphisms $\{f_n\}$ are uniformly κ-quasiconformal for some constant κ. Standard results in the theory of qausiconformal mappings then imply that this is a normal family, so any subsequence will have a further subsequence which converges uniformly on compact subsets of Ω to a candidate limit function f. We show that the domains and ranges of the f_n exhaust Ω and $\mathbf{D}$, respectively, so f is a homeomorphism of Ω onto $\mathbf{D}$. We appeal to the Key Lemma to prove that f is conformal, and conclude from our normalizations that this is the desired conformal (i.e., Riemann) mapping. Standard arguments show that the full sequence $\{f_n\}$ converges to f, completing the proof.

Quasiconformality: Let T be an open triangle forming a face of $\text{carr}\,(P)$ and $\widetilde{T}$ the corresponding open triangle in $\text{carr}\,(\widetilde{P})$. From its definition, the mapping $f_n : T \longrightarrow \widetilde{T}$ is affine; its dilatation on T is constant and easily computed. In particular, an upper bound on the dilatation of $f_n|T$ will follow if we demonstrate the existence of a positive lower bound on the angles of the triangles T and $\widetilde{T}$. For this we use one of the hypotheses on the packing P_n and the "ring lemma" of [26].

First, consider T: By hypothesis (c) of the Main Theorem, the ratio of (euclidean) radii of any two of the three circles forming T is bounded by $\mathfrak{C}_r$. In particular, the ratio of edge lengths is bounded by $\mathfrak{C}_r$, and the law of cosines easily yields a lower bound $\alpha > 0$ on the angles of T. For later use, note that hypothesis (d) of the Main

Theorem follows from (c): Any flower of carr (P_n) has non-overlapping petals, so the lower bound α on angles of faces gives the upper bound $2\pi/\alpha$ on the number of petals. Hereafter, $\mathfrak{d}$ will denote the integer part of $2\pi/\alpha$, and we see that no circle of P_n can have more than $\mathfrak{d}$ neighbors. (Note that these local comparisons of radii do not require the full strength of the hypothesis involving $\mathfrak{C}_r$.)

Next, consider $\widetilde{T}$: Here we argue in reverse by using $\mathfrak{d}$ and the ring lemma. A "chain" of circles is an ordered collection with each circle tangent to its predecessor.

Lemma 2.3.1 (Ring Lemma [26])**.** *Let c be a circle of euclidean radius ρ with a chain $\{c_1, \cdots, c_m\}$ of m circles externally tangent to c. Assume the circles have mutually disjoint interiors and the they precisely surround c, that is, c_m is tangent to c_1. There exists a constant τ depending only on m so that each circle c_j, $1 \leq j \leq m$ has euclidean radius at least $\tau\rho$.*

Proof: Given such a chain, assume without loss of generality that c_1 is the circle of the chain having largest radius. There is a uniform lower bound on this radius, namely, that which occurs with a chain of m equal-sized circles. The circle c_2 tangent to c_1 has a uniform lower bound for its radius; for if c_2 where extremely small, a chain of no more than $m-1$ circles starting from c_2 could not escape from the crevasse between c_1 and c in order to close up the chain. Repeating this reasoning for the circle c_3, c_4 and so forth, completes the proof. □

Now we apply this to $\widetilde{P}_n$: We have observed that a circle $\tilde{c}$ has at most $\mathfrak{d}$ neighbors. If $\tilde{c}$ is interior and $\tilde{c}_1$ is a petal of its flower, the Ring Lemma gives a uniform lower bound on the ratio of radius of $\tilde{c}_1$ to that of $\tilde{c}$. If $\tilde{c}$ is a boundary circle, a slight adjustment of the argument is necessary. Since $\tilde{c}$ is a horocycle, the petals of the flower stretch only part way around it, starting and ending with horocycles beside $\tilde{c}$. The argument for the ring lemma holds if we simply consider the outside of the unit disc as though it were another petal about $\tilde{c}$. From these considerations, we conclude that there is a bound, independent of n, on the ratios of the radii of any two circles forming $\widetilde{T}$. As with the bound α obtained for T, this gives a lower bound $\tilde{\alpha} > 0$ on the angles of $\widetilde{T}$. Together, α and $\tilde{\alpha}$ imply that the quasiconformal dilatation of the affine mapping $f_n|T$ is bounded by some constant κ for every face T (independent of n). Lastly, since f_n is continuous on carr (P_n) and since the edges form a set of Lebesgue area zero, a well known result from the theory of quasiconformal mapping (see [23, §V.3]) implies f_n is κ-quasiconformal throughout carr (P_n).

Exhaustion of $\mathbf{D}$*:* Each Andreev packing $\widetilde{P}_n$ has a simply connected carrier and boundary circles which are horocycles. Thus carr $(\widetilde{P}_n)$, the range of f_n, is starshaped with respect to the origin. To prove that these ranges exhaust $\mathbf{D}$, it suffices to show that the euclidean radii of the boundary circles go uniformly to zero as n goes to infinity. We use a "length-area" result from [26] and more of the strength of hypothesis (c).

Lemma 2.3.2 (Length-Area [26]). *Let c be a circle in $\mathbf{D}$ and let $S_1, S_2, \cdots, S_m$ be m chains of circles, each of which separates c (relative to $\mathbf{D}$) either from the unit circle or from the origin and a point of the unit circle. Assume that all the circles involved have mutually disjoint interiors. Denote the combinatorial lengths of the chains by $n_1, n_2, \cdots, n_m$. Then*

$$\textit{radius}\,(c) \leq (n_1^{-1} + n_2^{-1} + \cdots + n_m^{-1})^{-\frac{1}{2}}.$$

Proof: Suppose the chain S_j consists of circles of euclidean radius $\rho_{ji},\ 1 \leq i \leq n_j$. By the Schwarz inequality

$$\Big(\sum_i \rho_{ji}\Big)^2 \leq n_j \sum_i \rho_{ji}^2.$$

If $s_j = 2\sum_i \rho_{ji}$ is the geometric length of S_j, we have $s_j^2 n_j^{-1} \leq 4\sum_i \rho_{ji}^2$, implying

$$\sum_j s_j^2 n_j^{-1} \leq 4 \sum_{j\,i} \rho_{ji}^2 \leq 4.$$

Thus $s = \min\{s_1, s_2, \cdots, s_m\}$ satisfies

$$s^2 \leq 4(n_1 - 1 + n_2^{-1} + \cdots + n_k^{-1})^{-1}.$$

The separation conditions guarantee that s is greater than the diameter of c, so the above inequality proves the lemma. □

The hypotheses of the Main Theorem imply that as n goes to infinity the number of generations of circles separating the boundary circles of P_n from the origin goes to infinity. We simply need a way to count the number and lengths of separating chains. Fix n, and as before, let c_0 denote a circle of P_n whose flower contains the origin. Let d denote the infimum over all boundary circles c of the euclidean distance $\text{dist}(c, c_0)$ and write δ for mesh (P_n). Let m be the integer part of $(d - 2\delta)/4\delta$. We may assume without loss of generality that n is sufficiently large that m is positive.

Now fix a boundary circle c. For integers $j,\ 1 \leq j \leq m$, draw the circle L_j of radius $4\delta j$ concentric with c. It is easily seen that as one progresses in a fixed direction about L_j, the circles of P_n successively encountered will form one or more chains, each starting and ending with boundary circles. There may be several, since carr (P_n) could be quite irregular, but precisely one will separate c from c_0 within carr (P_n). Denote that chain by S_j. By hypothesis (c), its circles have radii no smaller than $\delta/\mathfrak{C}_r$. A moments reflection shows that at most $8j\mathfrak{C}_r\pi$ circles of this size and having mutually disjoint interiors could intersect L_j. Thus the combinatorial length n_j of S_j satisfies $n_j \leq 8j\mathfrak{C}_r\pi$. Finally, because the circles of P_n have radius no greater than δ, no circle of P_n can intersect both L_j and L_k for $j \neq k$; thus the chains S_j and S_k have no circles in common.

Moving over to $\widetilde{P}_n$, let $\widetilde{S}_j$ be the chain corresponding to $S_j,\ 1 \leq j \leq m$. Each $\widetilde{S}_j$ separates the circle $\tilde{c}$ from the origin (the center of $\tilde{c}_0$) within carr $(\widetilde{P}_n)$; more to the

point, $\widetilde{S}_j$ has ends which are horocycles, so it also separates $\tilde{c}$ from the origin and from some part of the unit circle within $\mathbf{D}$. By the Length-Area Lemma,

$$\text{radius}(\tilde{c}) \le (\sum_{j=1}^{m} n_j^{-1})^{-\frac{1}{2}} \le (\sum_{j=1}^{m} (8j\mathfrak{C}_r\pi)^{-1})^{-\frac{1}{2}} = \frac{2\sqrt{2\,\mathfrak{C}_r\pi}}{\sqrt{\sum_{j=1}^{m} j^{-1}}}.$$

This holds for every boundary circle $\tilde{c}$ of $\widetilde{P}_n$. Since the number of chains m goes to infinity as n grows, this bound goes to zero. Thus the euclidean radii of the boundary horocycles of $\widetilde{P}_n$ go uniformly to zero, implying that the ranges $\{\text{carr}\,(\widetilde{P}_n)\}$ exhaust $\mathbf{D}$.

Normal Family: We have shown that the simplicial mappings f_n are κ-quasiconformal homeomorphisms. By standard results in the theory of quasiconformal mappings [23, §II.5], $\{f_n\}$ is a normal family. Thus, any subsequence $\{f_{n_j}\}$ has a further subsequence which converges uniformly on compact sets to a κ-quasiconformal mapping f. Since their domains exhaust Ω and their ranges exhaust $\mathbf{D}$, the Carathéodory kernel theorem [23, §II.5] implies that f is a homeomorphism of Ω onto $\mathbf{D}$. We must argue that $f(0) = 0$ and that $f(x) > 0$.

Recall that c_0 is the circle of P_n whose flower contains the origin and that its counterpart $\tilde{c}_0$ is centered at the origin by our normalization of $\widetilde{P}_n$. By hypotheses (a) and (b) of the Main Theorem, the radius of c_0 goes to zero and the combinatoric distance between c_0 and the boundary circles of P_n goes to infinity as $n \to \infty$. In an argument similar to the above, one can find any number of mutually disjoint chains of circles from P_n which separate c_0 from the unit circle by taking n large; the corresponding chains in $\widetilde{P}_n$ separate $\tilde{c}_0$ from the unit circle. The Length-Area Lemma implies that the radius of $\tilde{c}_0$ goes to zero as $n \to \infty$. A similar argument with the circle c_x whose flower contains x shows that its counterpart $\tilde{c}_x$ has radius going to zero. Since $\tilde{c}_0$ is centered at the origin and $\tilde{c}_x$ on the positive real axis, we conclude that the limit function f satisfies $f(0) = 0$ and $f(x) \ge 0$. Since f is a homeomorphism, $f(x) > 0$.

Using the Key Lemma: If E is a compact subset of Ω, the Key Lemma tells us that as n goes to infinity, the dilatations of f_n on the interior of E go to 1. This means that the limit function f is 1-quasiconformal on $\text{int}\,(E)$, and since $E \subset \Omega$ is an arbitrary compact set, f is 1-quasiconformal on Ω. As is well known, this means f is analytic on Ω [23, §I.5].

We conclude that f is a one-to-one conformal mapping of Ω onto $\mathbf{D}$ with $f(0) = 0$ and $f(x) > 0$. It is an elementary consequence of the classical Schwarz Lemma that f is unique. The function f is also known as the Riemann mapping function for Ω, though the reader should note that we have established its existence without appeal to the Riemann Mapping Theorem. Now, since every subsequence of $\{f_n\}$ has a further subsequence converging to this f uniformly on compact subsets of Ω, the same holds

for the full sequence, and we have proven the first conclusion of the Main Theorem under the assumption that the Key Lemma holds.

3. Strategy for Proof of the Key Lemma

3.1. **Introduction.** The Key Lemma involves a comparison of P and $\widetilde{P}$. Though the details require the remainder of the paper, it is hoped that the fundamental ideas are accessible with the help of some computer-generated illustrations and a thought experiment. The experiment suggests an analogy between circle packings and electrical circuits which has been a continuous source of intuition for the author. Though originally quite vague — more a paradigm for random walks — it can now be seen as a rigorously faithful model for the dynamics of circle packings. Indeed, it seems sufficiently valuable that we return to it in Section 11, when the concepts are available for a fuller discussion. We start by reducing the proof of the Key Lemma to a study of individual angles in the carriers of our circle packings.

3.2. **A Reduction.** Here and in the sequel, the sequence of circle packings $\{P_n\}$ and associated simplicial mappings f_n will be as in the statement of the Main Theorem. Moreover, since our interest is in convergence on compact sets, we may, for the sake of convenience, fix $E \subset \Omega$ a compact Jordan region. For large n, $\mathrm{carr}\,(P_n) \supset E$, and to show that $f_n|E$ has dilatation close to 1, it suffices to show that a given face T of $\mathrm{carr}\,(P_n)$ lying in E is nearly similar to the corresponding face $\widetilde{T}$ of $\widetilde{P}_n$. This in turn will follow if the angles of T can be shown to be close to the corresponding angles of $\widetilde{T}$. Refer to Figure 2 where the typical situation is illustrated. Let ψ_n be an angle in a face of $\mathrm{carr}\,(P_n)$ which lies in E and let $\tilde{\psi}_n$ be the corresponding angle in the face of $\mathrm{carr}\,(\widetilde{P}_n)$. We may reduce the Key Lemma as follows:

Reduction 3.2.1. *The Key Lemma will follow if we can prove that given $\epsilon > 0$, there exists n_0 so that for packings P_n, $n > n_0$, the inequality $|\psi_n - \tilde{\psi}_n| < \epsilon$ holds for the angles ψ_n and $\tilde{\psi}_n$ as described above.*

3.3. **The Setting.** The jump from P to $\widetilde{P}$ — indeed, the very existence of $\widetilde{P}$ — is rather mysterious: one has this collection of radii for P which satisfy a complicated system of equations (reflecting the coherent pattern of circles); these are to be replaced by new radii satisfying an equally complicated system of equations, plus some side conditions which miraculously result in the boundary circles of $\widetilde{P}$ plotting as horocycles in $\mathbf{D}$. The existence of a clever algorithm which consistently solves this new system (a beautiful iterative scheme devised by Thurston [31]) only deepens the mystery. The algorithm provides fascinating imagery, circles jostling one another as some grow and some shrink, but it also proves frustrating because there is no way to see intermediate results — the configuration of circles does not fit together during the transition.

However, as P and $\widetilde{P}$ both lie in the unit disc, they may be treated as collections of circles in the hyperbolic (or Poincaré) metric. The situation immediately begins

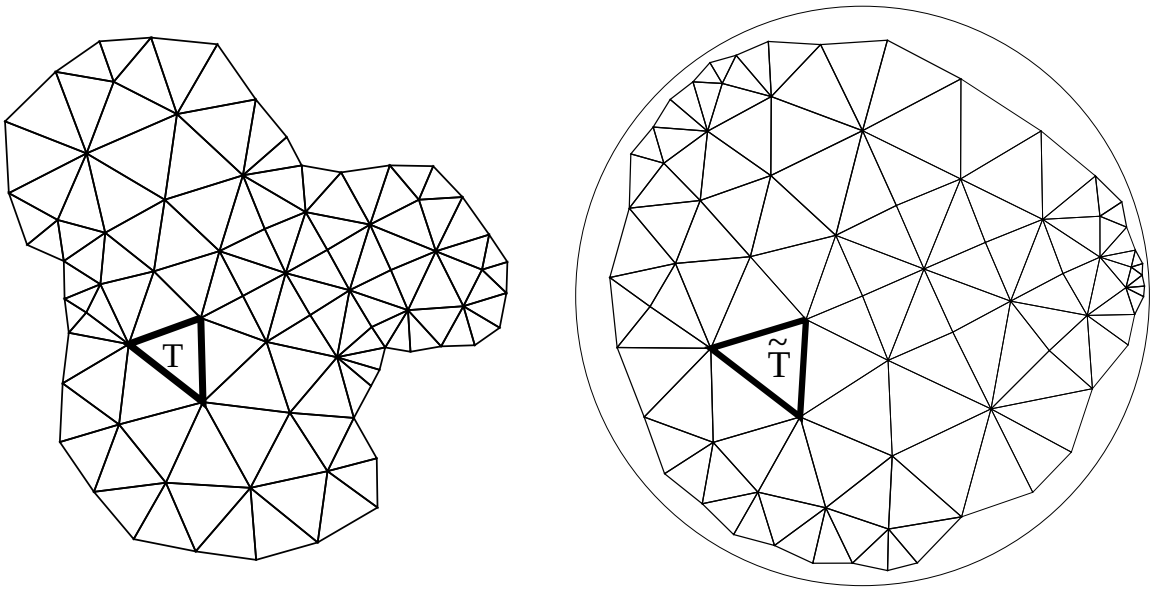

FIGURE 2. The carriers of P and $\widetilde{P}$.

to make much more sense. Now the horocycles of $\widetilde{P}$ represent hyperbolic circles of infinite radius, suggesting that the transition from P to $\widetilde{P}$ can be treated as some type of continuous phenomenon in which the boundary circles increase to infinity in radius. That is precisely what we do — we parameterize the coherent circle packings associated with a given complex *via* their hyperboic radii and define in this parameter space a path in from P to $\widetilde{P}$ which is not only continuous, but differentiable. The angle ψ of interest in proving the Key Lemma becomes a differentiable function so that the bound on $|\psi - \tilde{\psi}|$ can be obtained by integrating the differential $d\psi$. Our problem is then reduced to proving that $d\psi$ remains small along this path if the mesh of P is small to begin with.

The sequence of images in Figure 3 illustrates steps in the progression from the packing on the left of Figure 1 to its Andreev packing, on the right in Figure 1. (An even more dramatic display of the overall behavior can be seen if a finer sequence of steps is computed and displayed *via* computer animation.) It is difficult to judge hyperbolic radii from the pictures, but in fact all circles are increasing in this progression. Indeed, what pushes the packing towards $\widetilde{P}$ is a steady forced increase in boundary radii towards infinity.

Helpful as these pictures may be, it is actually the jostling of circles — the dynamics — occurring **between** successive frames which concerns us most. Estimates on ψ require a thorough understanding of how incremental (think "differential") increases in boundary circles have an effect which ripples through to the interior circles. The pivotal insights into our approach lie with this dynamic process; we pose a thought experiment suggesting that it is reminiscent of a random walk. First, some comments

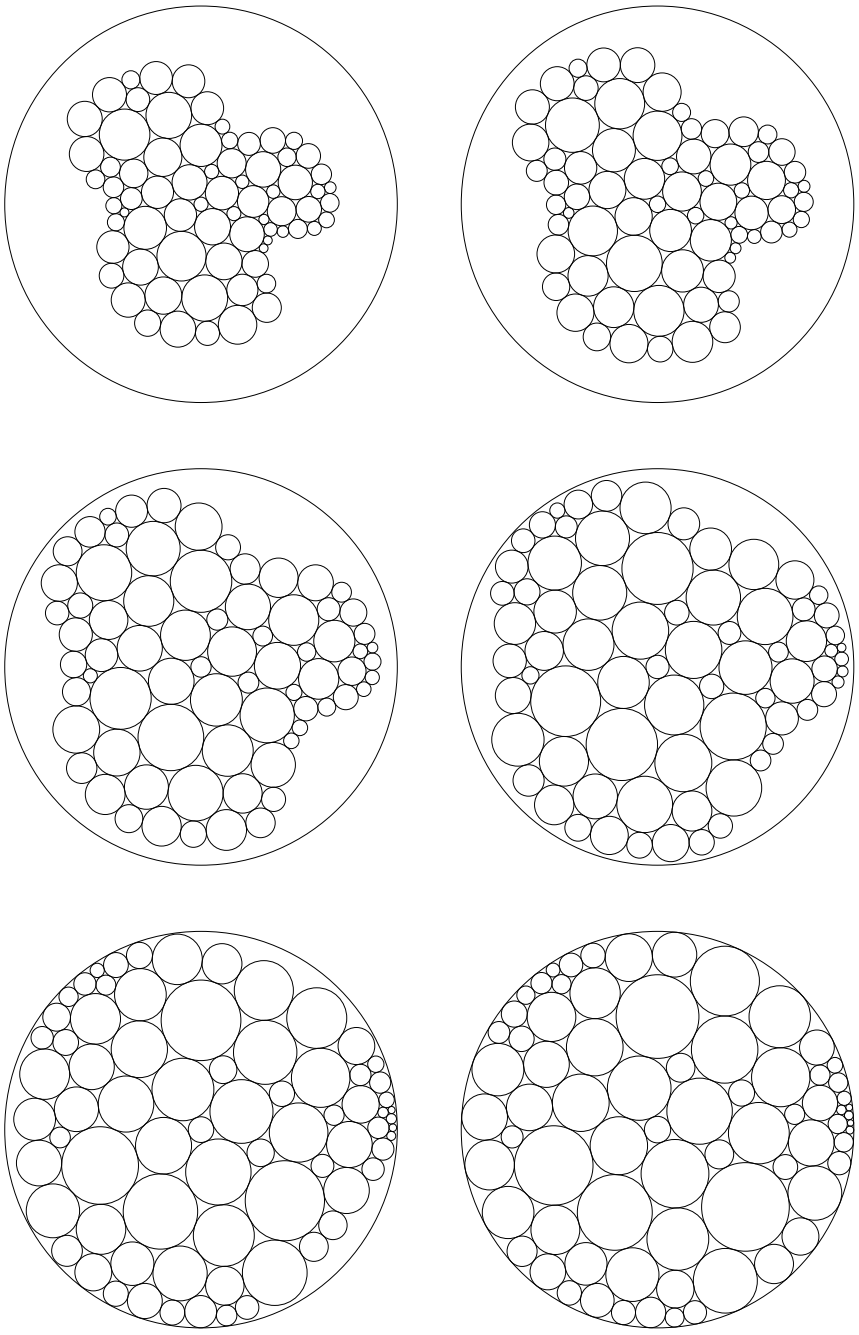

FIGURE 3. A progression of packings from P to $\widetilde{P}$.

about angles: at each circle in a packing there are several angles formed by the geodesics from (the center of) that circle to its neighbors. Adding these angles together gives

that circle's **angle sum**. An interior circle will be properly packed if its angle sum is 2π. In our experiment, it is important to notice that when a circle increases in radius, its angle sum decreases, while the angle sums of its immediate neighbors increase. In manipulating a circle packing, it is the radii which we will be adjusting, but the angle sums which we monitor for compliance with packing conditions.

3.4. **An Experiment.** We rely on the notation of Figure 4; note that we are in the hyperbolic setting, using hyperbolic centers, radii, geodesics, and so forth. Our experiment involves increasing the radius of the single boundary circle C_1 and watching the resulting effects. (C_1 is labelled "1" in Figure 4. The amount it changes will be large for purposes of illustration, but should be thought of as an infinitesimal increase in hyperbolic radius.) The angle sum at C_1 is made smaller by this change, and the aim of the experiment is to accommodate this new angle sum.

> *OJBECTIVE: We want to adjust the radii of P in order to realize a specified change in angle sum at C_1, while maintaining the original angle sums for all other circles (both interior and boundary).*

Because of the initial increase in C_1, the neighboring circles feel uncomfortable — each now finds itself with an angle sum which is larger than desired. Take C_2, for example: its angle sum now exceeds 2π and its petals stretch too far around it. To reestablish its local packing condition, C_2 changes its radius — in fact, it is clear that C_2 must increase to push those neighbors apart again. Of course, the action of C_2 makes its neighbors uncomfortable: C_1 loses a bit of the decrease in its angle sum which it is trying to maintain; C_3 and C_4, with angle sums already too large due to C_1, are made worse; other neighbors, such as C_5, begin to feel the effects for the first time. Suppose next that C_3, say, increases to reestablish its original angle sum. This in turn puts upward pressure on its neighbors; these neighbors adjust; that puts pressure on their neighbors; and so forth and so on, *ad infinitum*. It is clear that the initial impulse due to the change in C_1 reverberates throughout the pattern of circles, driven by an infinite process of adjustment and readjustment of radii.

Does this process converge to give a new collection of radii? All adjustments involve increases in radii, but since we are working at the differential level, this alone won't imply convergence. We will see shortly, however, that there are effects on hyperbolic area which guarantee that the process will ultimately die out. The final accumulated increases in radii result in a new collection of radii which incorporates the desired angle sum decrease at C_1. The final configuration is shown on the right in Figure 4 — notice that we don't try to show the intermediate stages, since there is no consistent way to plot the pattern of circles until the interior angle sums are back to 2π.

Readers familiar with Markov chains or random walks may sense a similar phenomenon here. A concrete model which serves as a convenient paradigm is the electrical circuit, though we can suggest the analogies only informally at this stage: The vertices of the abstract complex K for the circle packing serve as nodes in the circuit, the edges

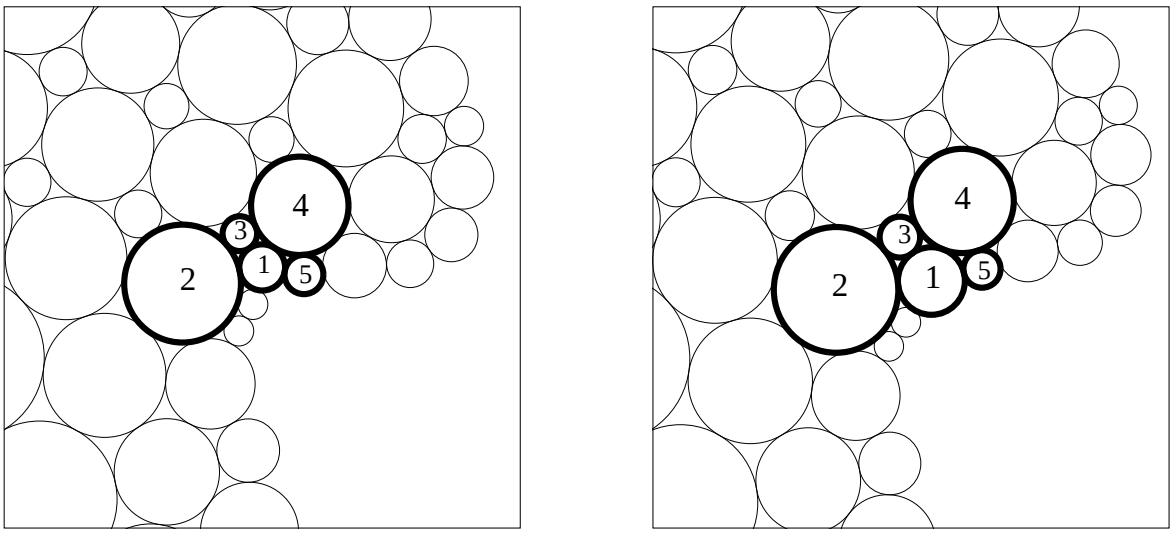

FIGURE 4. The experimental setting.

as wires, each of some resistance. In the experiment above, a "charge" is placed at a single boundary node and then moves about the circuit as would an electrical current. Current arriving at a node moves to the neighbors in certain proportions, based on the relative resistances of the wires. More picturesquely, one can imagine an individual electron arriving at a node, randomly choosing among the available wires, with probabilities based on the resistances, and moving along the chosen wire to its next stop. In this viewpoint, the overall behavior of the circuit simply reflects the averaged behavior of large numbers of individual electrons.

(a). *What is the "current"?* When a circle increases, its angle sum drops while that of each neighbor goes up; in essense, some quantity of angle has been sent from its node to each of its neighboring nodes along edges of the network. This moving angle, to be termed **curvature**, comprises the current, and it is driven by changes in radii. The initial "charge" at C_1 represents the amount of angle to be removed from the angle sum at C_1, and the process starts by increasing C_1 to accomplish this. The process continues because no circle is permitted to end up with any excess curvature; each circle receiving curvature must increase in radius in order to disperse it.

(b). *Where is the "ground"?* In fact, curvature won't bounce around forever. In hyperbolic geometry, angles and area are intimately connected. When a circle radius increases, the area of each of its faces in the packing will increase. Consequently, part of the curvature driven away by a radius

increase is shuttled to the neighbors, while part goes into area. (In fact, since the area of a triangle is π minus the sum of its angles, elementary geometric arguments show that 100% of the curvature is accounted for in this way.) But curvature absorbed as area will no longer affect the process, since it does not necessitate the correction of any angle sum — in essense, it has reached ground. Thus, though no nodes are grounded in the usual sense, every node has a "leakage" to ground. Each electron ("quantum" of curvature) pumped in at C_1 will bounce around the circuit until it finally leaks to ground at some node.

(c). *What is "resistance"?* Resistance of an edge depends entirely on the local geometry and, as with electricity, somehow measures the ease with which curvature flows — in §6 we actually compute its reciprocal, termed conductance. The ease with which curvature flows into the area of faces is related to the leakage, and this is a particularly important aspect of the model: In euclidean geometry, angles and area are not connected — all angle changes would flow to neighbors, and leakage would be zero. Although we work in hyperbolic geometry, when a circle and its neighbors are very small, the triangle they form is nearly euclidean, and leakage will be close to zero (justifying its name).

We have not mentioned voltage: using Ohm's Law, voltage may be inferred from the currents and conductances, and in fact plays a central role later. Property (b) above guarantees that the infinite process of radius adjustment which we have described will finally run its course, the initial charge at C_1 will have leaked to ground among the various nodes, and one can read off the results. Leakage at each node is associated with radius increases there; hence the various leakage totals reflect precisely the accumulated radius adjustments to the corresponding circles. When all this is quantified, the model should provide the changes in radii needed to accommodate precisely the decreased angle sum at C_1.

CONCLUSION: We expect to model the dynamics of a circle packing with a Markov process, and thereby determine the changes in radii necessary to realize a specified change in angle sum at C_1.

Fortunately, this all does in fact work, and we are in position to see in general terms how to use this model. In the hyperbolic setting, $\widetilde{P}$ is characterized among the coherent circle packings sharing its complex K by having all its boundary angle sums zero (i.e., having horocycles as boundary circles). To move continuously from P to $\widetilde{P}$, we therefore arrange a continuous decrease of boundary angle sums to zero. At each (infinitesimal) stage, the desired angle sum decreases represent a charge distributed on the boundary of K (just as with the single charge at C_1 above). Our Markov model shows how this charge distributes itself about the complex, and this allows computation

of the requisite changes in circle radii — in particular, it allows estimates of the change in the angle ψ (see §3.2.1) from the amount of curvature leaked at the three nodes (i.e., circles) forming it.

When P nearly fills Ω and has very small mesh, one can make some qualitative judgements about the distribution of curvature, and hence about the changes in ψ, at each stage in the move from P to $\widetilde{P}$: First, the nodes associated with ψ are deep in the interior of K, so any mal-distribution of the initial charge on the boundary will moderate before it affects ψ. Second, and more important, as suggested in (c) above, the leakage probabilities are very small — a quantum of curvature will experience many transitions from node to node before finally leaking to area. Both these features suggest that the current will approach some type of steady state distribution. In particular, neighboring nodes deep in the interior would be expected to have only very small **net** current between them (amount going one way minus that going the other). It is precisely the net current which affects ψ — after all, the current represents moving angle. This, then, is the central intuition provided by the model:

> *INTUITION: Small mesh for P means small net movement of curvature deep inside K as the radii move towards their Andreev values, and this means small net change in ψ.*

3.5. **Outline.** It is hoped that this description of the model will sustain the reader during the proof, which requires the next seven sections of the paper.

Section 4 begins with preliminary material on hyperbolic geometry, introduces useful auxiliary functions, and establishes some of the basic monotonicity results for circle configurations in the hyperbolic plane. Sections 5–7 are devoted to a thorough study of a given circle packing P and related packings sharing its complex K: In §5 we place hyperbolic structures on K corresponding to circle packings and define a parameterized path of such structures running from P to $\widetilde{P}$. In §6 we introduce the Markov processes which model curvature flow within each such structure; we compute transition probabilities and conductances; and we review basic notions in the study of random walks. In §7 we apply the model to compute the differential changes in radii on the way to $\widetilde{P}$, and we arrive finally at a certain nonnegative discrete harmonic function which describes the ultimate effects of those differential changes.

It is not until Sections 8 and 9 that the geometric hypotheses of the Main Theorem enter: In §8, we make those hypotheses explicit and we establish preliminary geometric estimates. In §9 we state and prove a discrete version of a classical Harnack inequality. It quantifies the "evenness" with which curvature is distributed, as mentioned earlier. The underlying intuition is that for large complexes, the associated electrical circuits approach in behavior an infinite, regular electrical grid. These infinite grids are reasonably well understood due to work of Pólya.

That brings us finally to the proof of the Key Lemma in Section 10. In the author's view, this is where the deeper connections between the Markov processes and the geometry of circle configurations come into play. Until this point, the random walks might be considered as mere computational devices; but they become indispensible in §10, with some very pleasing identities relating hyperbolic geometry, electrical resistance, and random walks. The technical details are rather involved, but we try to bring out the intuition behind them when we reprise the electrical analogy in Section 11.

4. Hyperbolic Geometry and Computations

4.1. **Introduction.** Our proof of the Key Lemma is carried out largely in hyperbolic rather than euclidean geometry — an essential rigidity present in the hyperbolic setting plays a central role in the developments. For basic facts regarding hyperbolic geometry and trigonometry, we refer the reader to [4]. In this section we recall some of these while establishing notation. We also introduce useful auxiliary functions and prove fundamental estimates and identities which will be required in the sequel.

4.2. **The Hyperbolic Plane.** The unit disc $\mathbf{D}$ will serve as our model of the hyperbolic plane when it is endowed with the Poincaré metric

$$ds = 2|dz|/(1 - |z|^2),$$

which has constant curvature -1. The geodesics are arcs of circles which are orthogonal to the unit circle. Circles in the Poincaré metric are euclidean circles in $\mathbf{D}$, though centers and radii are hyperbolic quantities. Horocycles, euclidean circles which are internally tangent to the unit circle, may be construed in a natural way (see [4]) as hyperbolic circles having infinite radius — centers are the ideal boundary points corresponding to their points of tangency with the unit circle. Note in particular that with this convention, the geodesic segment between centers of tangent circles (whether regular circles or horocycles) will pass through their point of tangency. The orientation preserving rigid motions of the hyperbolic plane are the conformal automorphisms (Möbius transformations) of $\mathbf{D}$. As isometries in the hyperbolic metric, they map finite circles to finite circles, horocycles to horocycles, and geodesics to geodesics.

Quantities involved in the Main Theorem, such as $\mathfrak{C}_r$ and $\mathrm{mesh}(\,\cdot\,)$, are euclidean, while it is generally hyperbolic information which is needed in the proofs. One switches between the two by using the Poincaré density. For instance, the euclidean distance ρ and the hyperbolic distance r of a point from origin are related by

$$\rho = \frac{e^r - 1}{e^r + 1}.$$

Within compact subsets of $\mathbf{D}$, hyperbolic and euclidean distances are comparable; specifically, if $0 < \tau < 1$, the hyperbolic radius r and the euclidean radius ρ of a circle

in $\{|z| \leq \tau\}$ satisfy

$$\rho \leq r \leq \frac{2\rho}{1-\tau^2}.$$

In several instances we use the fact that for circles centered at the origin, an inequality involving their hyperbolic radii will persist for their euclidean radii. We will say two circles are **comparable with constant** $C > 1$ if their hyperbolic radii r_1, r_2 satisfy $r_1/C \leq r_2 \leq r_1 C$.

Some feel for differences and similarities between hyperbolic and euclidean geometry will be useful for our later work. In the large, there is much more room near infinity in the hyperbolic plane — which in some measure explains why it has a richer geometry and supports a richer analytic function theory. Thus, the circumference of a circle grows much faster relative to its area in the hyperbolic setting than in the euclidean. As but one consequence, we note the following fact which will be useful later:

Lemma 4.2.1 ([6]). *Let c be the central circle in a flower having n petals lying in the hyperbolic plane and assume c has hyperbolic radius r. Then $r \leq \sqrt{n}$.*

This fails in the euclidean setting, where a flower can be scaled by an arbitrarily large factor and remain a flower.

Also, as a consequence of its negative curvature, hyperbolic geometry enjoys a certain rigidity which is not present in euclidean geometry. This is reflected in the following connection between angles and hyperbolic area, which is fundamental for our work:

Lemma 4.2.2 (Area Rule). *If T is a hyperbolic triangle with angles α, β, γ, then its hyperbolic area is given by*

$$\mathit{Area}(T) = \pi - (\alpha + \beta + \gamma).$$

At one extreme, no triangle has area greater than π. This area is achieved by an "ideal triangle", that is, one with vertices at ideal boundary points and hence zero angles. On the other hand, if the area is extremely small, then the angles add to nearly π, suggesting that small triangles are approximately euclidean.

A basic observation is that to any triple $a, b, c \in (0, \infty]$ there corresponds a triple of mutually and externally tangent circles having hyperbolic radii a, b, c; this configuration of circles is unique up to rigid motions of the hyperbolic plane. Let T be the hyperbolic triangle formed by the centers of the circles. It is in this setting that we state the hyperbolic cosine rule:

Lemma 4.2.3 (Cosine Rule). *Assume T is formed by a mutually tangent triple of circles having hyperbolic radii a, b, c. Let α be the angle of T at the center of the circle of radius a. Then*

$$\cos\alpha = \frac{\cosh(a+b)\cosh(a+c) - \cosh(b+c)}{\sinh(a+b)\sinh(a+c)}.$$

Actually, a triple of circles determines two triangles, one using hyperbolic centers and edges, another using euclidean. (In either setting, every triangle will arise from a triple of circles in this way, and the radii are unique and easily computed.) The next result expresses again that hyperbolic geometry is infinitesimally euclidean.

Lemma 4.2.4. *Let c_1, c_2, c_3 be a mutually tangent triple of circles lying in the compact set $\{|z| \leq \tau\}$ for some $\tau \in (0,1)$. Let T and T^h be the triangles formed by their euclidean and by their hyperbolic centers, respectively, and let α_j, α_j^h, $j = 1,2,3$, denote their angles. Given $\epsilon > 0$, there exists $\sigma > 0$, depending on τ only, so that if the hyperbolic diameter of T^h is less than σ, then $|\alpha_j - \alpha_j^h| < \epsilon$, $j = 1,2,3$.*

The proof is elementary, relying on the fact that in a compact subset of $\mathbf{D}$ and for small circles, the hyperbolic centers are close to the euclidean centers and the hyperbolic geodesic edges are close to euclidean segments; the details are left to the reader.

4.3. **Radius Variables and Auxiliary Functions.** Our interest for the remainder of this section lies with computations required in the sequel and involving hyperbolic radii, angles, and areas. The expressions encountered are easier to manipulate and often more transparent using an alternate variable:

Definition 4.3.1. *Let r represent the hyperbolic radius of a circle (i.e., the radius in the Poincaré metric), $0 < r \leq \infty$. We will define a special radius, referred to as an* ***s-radius****, via $s = \exp\{2r\}$. Note that s is strictly increasing in r and $1 < s \leq \infty$.*

In the sequel, we revert to the variable s in most computations, generally without comment. Indeed, we abuse terminology further by using the same symbol to designate both a circle and its s-radius — the context should make the meaning clear. As an example, let A denote the hyperbolic area of the triangle formed by vertices v, u, w of Figure 5. If r denotes the hyperbolic radius of the circle at v, we have $\dfrac{\partial A}{\partial r} = \dfrac{\partial A}{\partial v}(2v)$, where $\dfrac{\partial A}{\partial v}$ denotes the derivative with respect to s-radius $v = e^{2r}$. Note that if two circles are comparable with constant C (see above), then their s-radii s_1, s_2 satisfy $s_1^{1/C} \leq s_2 \leq s_1^C$, and conversely.

Auxiliary Functions 4.3.2. Assume the variables x, y, z, s, t have domain $(1, \infty)$. Define the auxiliary function

$$g(x,y,z) = \arccos\Big[\frac{(xy+1)(xz+1) - 2x(yz+1)}{(xy-1)(xz-1)}\Big].$$

Its partials are given by

$$g_1(x,y,z) = \frac{\partial g}{\partial x}(x,y,z) = \frac{-(x^2yz-1)\sqrt{(y-1)(z-1)}}{(xy-1)(xz-1)\sqrt{x(x-1)(xyz-1)}}$$

$$g_2(x,y,z) = \frac{\partial g}{\partial y}(x,y,z) = \frac{\sqrt{x(x-1)(z-1)}}{(xy-1)\sqrt{(y-1)(xyz-1)}}$$

$$g_3(x,y,z) = \frac{\partial g}{\partial z}(x,y,z) = \frac{\sqrt{x(x-1)(y-1)}}{(xz-1)\sqrt{(z-1)(xyz-1)}}.$$

Define the auxiliary function

$$h(x,s,t,y) = \frac{\sqrt{x(x-1)}}{(xy-1)\sqrt{y-1}}\Big[\frac{\sqrt{s-1}}{\sqrt{xys-1}} + \frac{\sqrt{t-1}}{\sqrt{xyt-1}}\Big].$$

Observe that after rearrangement, $h(x,s,t,y) = g_3(x,s,y) + g_3(x,t,y)$.

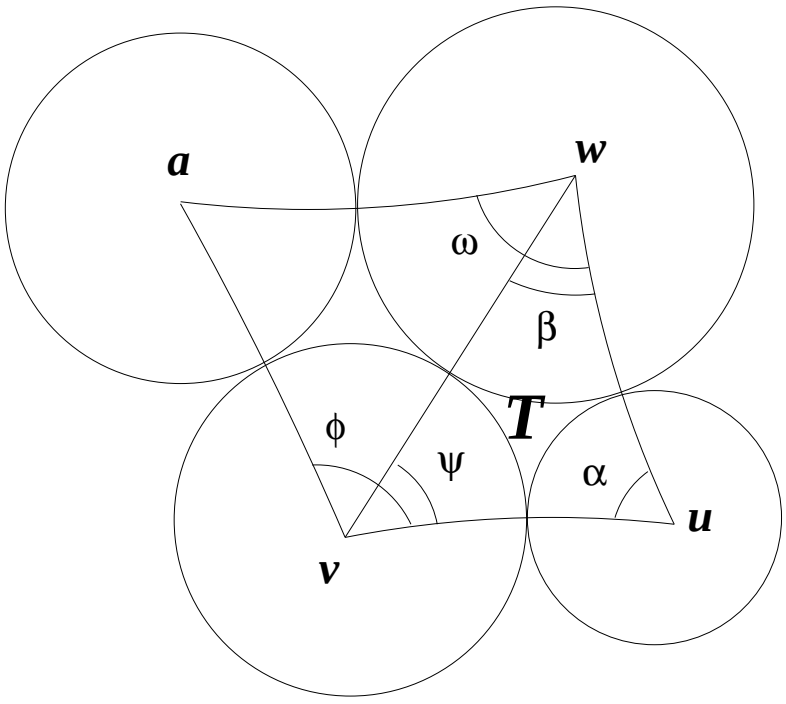

FIGURE 5. Setting for computations.

The connections between these functions and hyperbolic geometry are established using the Cosine and Area Rules. Refer to the limited configuration of circles of

Figure 5, which shows contiguous hyperbolic triangles formed by the four circles v, u, w, and a, with various angles of interest labelled. The hyperbolic triangle formed by v, u, w is denoted T and has hyperbolic area A. Note that one (or more) of the circles could be horocyles. Using the s-radii of the circles, we have:

$$\psi = g(v,u,w), \qquad \alpha = g(u,v,w), \qquad \beta = g(w,u,v),$$

$$A = \text{Area}(T) = \pi - g(v,u,w) - g(u,v,w) - g(w,u,v),$$

$$\frac{\partial \psi}{\partial v} = g_1(v,u,w), \qquad \frac{\partial \phi}{\partial v} = g_1(v,u,w) + g_1(v,w,a), \qquad \frac{\partial \omega}{\partial v} = h(w,u,a,v).$$

There are several beautiful identities involving these functions; particularly important for later use are these — verification is left to the reader.

$$\frac{g_2(u,v,w)}{g_2(v,u,w)} = \frac{h(u,a,w,v)}{h(v,a,w,u)}\,, \qquad \frac{g_3(w,u,v)}{g_3(v,u,w)} = \frac{h(w,a,u,v)}{h(v,a,u,w)}\,. \tag{1}$$

4.4. **Computations.** Many of the results here are geometrically intuitive; however, we restict ourselves to the computations and discuss the geometry when it is more helpful later.

Lemma 4.4.1. *Let x, y, z, s, t be variables with domain $(1, \infty)$. Then*

(i). $g_1(x,y,z) < 0, \quad g_2(y,x,z) > 0, \quad g_3(z,y,x) > 0.$

If x, y, z, s, t are pairwise comparable with constant $C > 1$ and all are bounded above by constant $B \in (1, \infty)$, then there exist constants C_1, C_2 and $C_3 > 1$, depending on C and B only, so that the following inequalitites hold:

(ii). $|\dfrac{g_2(y,x,z)}{g_1(x,y,z)}| \le C_1.$

(iii). $|g_1(x,y,z)\sqrt{x}(x-1)| \le C_2.$

(iv). $C_3^{-1} < h(y,s,t,x)\sqrt{x}(x-1) \le C_3.$

Proof: The inequalities of (i) are immediate from the earlier expressions for the partials of g. (Recall that s-radii always exceed 1.) Regarding (ii), after rearrangement we have

$$0 < -\frac{g_2(y,x,z)}{g_1(x,y,z)} = -\sqrt{xy}\,(\frac{xz-1}{x^2yz-1}).$$

Comparability of the arguments implies $y^{1/C} \le x \le y^C$, and $z^{1/C} \le x \le z^C$, so

$$|\frac{g_2(y,x,z)}{g_1(x,y,z)}| \le x^{1+C/2}\big(\frac{x^{1+c}-1}{x^{2+2/C}-1}\big).$$

Since the arguments are bounded above, we need only concern ourselves with small values of x, and L'Hôpital's rule shows that this goes to a positive limit as $x \downarrow 1$. The computations for (iii) and (iv) are substantially the same and are left to the reader. □

Lemma 4.4.2 (Monotonicity [6]). *Let T be the triangle of Figure 5 and assume the associated s-radii v, u, w are finite. Then the angle ψ is strictly decreasing in v and strictly increasing in u and w; the hyperbolic area is strictly increasing in v.*

The monotonicity of angles follows from Lemma 4.4.1(i); the monotonicity of area is best verified geometrically. Indeed, the expression for the partial derivative of area is

$$\frac{\partial A}{\partial v} = -\frac{\partial \psi}{\partial v} - \frac{\partial \alpha}{\partial v} - \frac{\partial \beta}{\partial v}$$

$$= \big(\frac{\sqrt{(u-1)(w-1)}\,\big[\,(v^2uw-1)-(wv-1)\sqrt{uv}-(uv-1)\sqrt{wv}\,\big]}{(vu-1)(vw-1)\sqrt{v(v-1)(uvw-1)}}\big),$$

and its positivity is difficult to verify by direct computation. For details, the reader is referred to [6], where monotonicity plays the central role. There, for example, additional expressions are established for ψ and A when one or more of the circles forming T has infinite radius; we find it easier to avoid those cases in this paper.

Our last result simply states that when the circles forming T are small, then the rate of change of area with respect to s-radius is small.

Lemma 4.4.3. *Let A denote the hyperbolic area of the triangle T of Figure 5, and treat it as a function of v alone, with u and w fixed. If the s-radii v, u, w are bounded above by constant $B \in (1, \infty)$, then there exists a constant C_4, depending on B only, so that*

$$\frac{dA}{dv} \le C_4.$$

Moreover, $C_4 \longrightarrow 0$ as $B \downarrow 1$.

Proof: If r represents the hyperbolic radius associated with the s-radius v, then

$$\frac{dA}{dv} = (\frac{dA}{dr})(\frac{1}{2v}) \le (\frac{1}{2})\,\frac{dA}{dr}.$$

For convenience, place one vertex of T at the origin. Note that for B close to 1, T will lie in a small neighborhood of 0, and in that neighborhood the Poincaré density is approximately 2. That is, hyperbolic distances and areas are comparable to euclidean distances and areas; the result then follows from the result for euclidean radii and areas — e.g., by Heron's formula. □

5. Parameterization of Packings

5.1. **Introduction.** Throughout this and the next two sections, P will represent an arbitrary but fixed circle packing with DL-complex K and Andreev packing $\widetilde{P}$. Here we establish definitions and notations, and describe the "hyperbolic structures" on K which were introduced in [6] to represent circle configurations. These structures allow the parameterization of circle packings and thereby the description of a curve in parameter space corresponding to a continuous deformation of P to $\widetilde{P}$.

5.2. **Hyperbolic Complexes.** The oriented 2-complex K encodes the combinatorics of the circle packing P (and of $\widetilde{P}$), but contains no information about the circles themselves. We rectify this by employing hyperbolic complexes:

Let $\{v_1, v_2, \cdots, v_k\}$ denote the vertices of K. The order will be fixed, with the first q being the boundary vertices, and the remaining p the interior vertices, $q > 0,\ p > 0,\ k = q + p$. If we specify a vector $\mathbf{r} = [r_1, r_2, \cdots, r_k]$ of real numbers, one for each vertex, then the resulting object is termed a **hyperbolic complex** and will be denoted $K(\mathbf{r})$. The coordinate r_j is to be thought of as the hyperbolic radius of a circle associated to vertex v_j; boundary radii may be infinite, so $0 < r_j \leq \infty,\ 1 \leq j \leq q$, but we assume interior radii are finite, $0 < r_j < \infty,\ q < j \leq k$. As an example, and for later use, we have the

Definition 5.2.1. *Denote by R the vector of hyperbolic radii taken from the circle packing P and by $\widetilde{R}$ the vector of hyperbolic radii taken from $\widetilde{P}$.*

The hyperbolic complexes $K(R)$ and $K(\widetilde{R})$ contain all the information about P and $\widetilde{P}$, respectively, up to automorphisms of $\mathbf{D}$.

Of course, for a randomly chosen vector of radii $\mathbf{r}$, $K(\mathbf{r})$ will not, in general, be associated with a coherent configuration of circles. Nonetheless, $K(\mathbf{r})$ does have a hyperbolic structure, which we may briefly describe as follows: Any ordered triple of hyperbolic radii determines an (counterclockwise) oriented triple of mutually and externally tangent circles in $\mathbf{D}$ which is unique up to rigid motions, and the circle centers determine a unique hyperbolic triangle. If the three radii are components of $\mathbf{r}$ associated with the vertices of a face f of K, then the hyperbolic structure on the triangle in $\mathbf{D}$ can be lifted to f. Since faces sharing an edge e of K can be laid down so that they share an edge in $\mathbf{D}$, the structures lifted to the faces are compatible across e. We conclude that by lifting triangular structures face-by-face, the radii of $\mathbf{r}$ determine a hyperbolic structure throughout K, with the possible exception of singularities at interior vertices. It is this structure which justifies the name hyperbolic complex for $K(\mathbf{r})$ and allows for measurement of areas, angles, and distances.

Particularly important are the angles of the faces of $K(\mathbf{r})$, each of which can be computed *via* the Cosine Law using the three radii associated with the face. For a vertex v_j, the sum of the angles at v_j in the faces of $K(\mathbf{r})$ to which v_j belongs is termed the **angle sum** at v_j. Of course, this angle sum does not depend on all the radii of the

vector $\mathbf{r}$, only on r_j and the radii for vertices neighboring v_j. If the radii in the vector $\mathbf{r}$ are associated with a coherent configuration of packed circles, then it is immediate that the angle sum at each interior vertex v_j must be 2π; only in this way will circles for v_j and its neighbors fit precisely together to form a flower in the hyperbolic plane. That leads to the following

Definition 5.2.2. *In the hyperbolic complex $K(\mathbf{r})$, the angle sum at a vertex v_j is denoted $\theta_j = \theta_j(\mathbf{r})$. $K(\mathbf{r})$ is termed a **packing** if $\theta_j = 2\pi$ for every interior vertex v_j.*

These ideas are developed fully in [6], so we will not go into great detail here. A few points should be highlighted, however. One can attempt to lay out the hyperbolic complex $K(\mathbf{r})$ in $\mathbf{D}$ by placing an initial face (formed by a mutually tangent triple of circles with radii from $\mathbf{r}$), laying down another face sharing an edge with the first, and so forth, until all faces are placed. This will be successful only for packings.

Proposition 5.2.3 ([6])**.** *There exists a well defined (orientation preserving) locally isometric immersion of the hyperbolic complex $K(\mathbf{r})$ into the hyperbolic plane if and only if $K(\mathbf{r})$ is a packing. In this case the immersed image is unique up to rigid motions of $\mathbf{D}$.*

As an example, consider the hyperbolic complex $K(R)$ associated with P. In its immersed image, the vertices of K will (after an appropriate rigid motion) be mapped to the hyperbolic centers of the corresponding circles of P. This image forms the "hyperbolic carrier" of P. Similarly, an immersion of $K(\widetilde{R})$ forms the hyperbolic carrier of $\widetilde{P}$. These are illustrated in Figure 6 (compare to the carriers for these packings in Figure 2). Note that these two immersions happen to be embeddings, since they are globally one-to-one; this will not necessarily be the case for the typical intermediate packings we encounter. (For an illustration, see Figure 7 of [6].)

The parameter space we use is the space of admissible radius vectors,

$$\mathbf{r} = [r_1, \cdots, r_q \ ; \ r_{q+1}, \cdots, r_k] \in (0, \infty]^q \times (0, \infty)^p \ ,$$

and will be denoted by $\mathfrak{R}$. For any $\mathbf{r} \in \mathfrak{R}$, the hyperbolic complex $K(\mathbf{r})$ determines a vector $[\theta_1, \cdots, \theta_q \ ; \ \theta_{q+1}, \cdots, \theta_k]$ of angle sums for the vertices of K. It is a convenience in these notations to use a semicolon between the first q and the last p coordinates, demarking the distinction between boundary and interior data, respectively.

Definition 5.2.4. *Given K, the mapping from the vector $\mathbf{r} \in \mathfrak{R}$ to the corresponding vector of angle sums will be called the **angle sum map** and will be denoted Θ,*

$$\Theta(\mathbf{r}) = [\theta_1(\mathbf{r}), \cdots, \theta_k(\mathbf{r})].$$

Each angle sum θ_j is nonnegative and strictly less than π times the degree of the vertex v_j; $\theta_j = 0$ if and only if v_j is a boundary vertex and $r_j = \infty$. It appears that the precise range of the angle sum map depends in subtle ways on the combinatorics of K, an issue which does not concern us here. Whatever that range, we will call it $\mathfrak{A}$; this is our "angle space", while $\mathfrak{R}$ is our "radius space". Let $\mathfrak{S}^\infty$ denote the intersection of

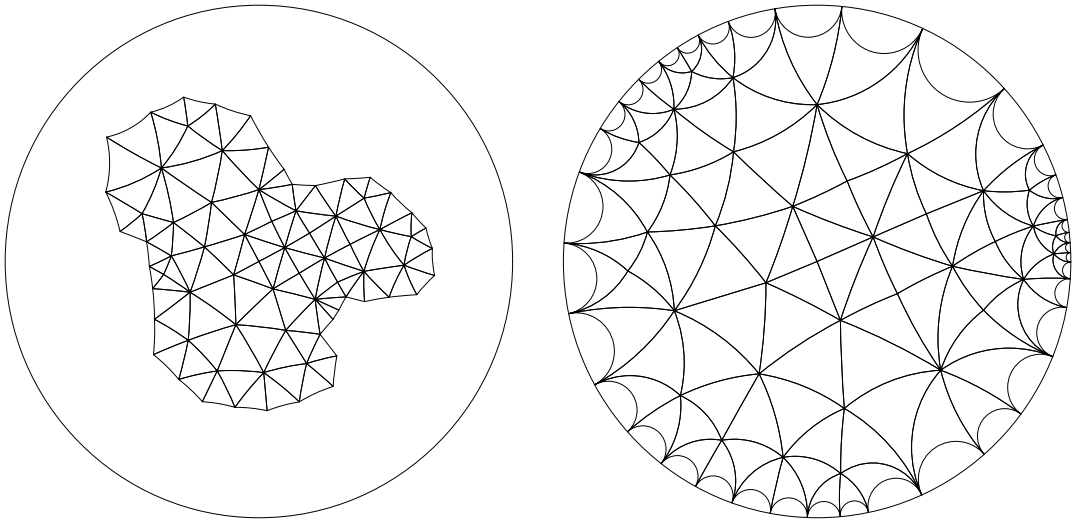

FIGURE 6. Immersions of $K(R)$ and $K(\widetilde{R})$.

$\mathfrak{A}$ with the affine subspace of vectors whose last p coordinates are 2π. By definition, $\mathfrak{S}^\infty$ consists of angle sums associated with packings $K(\mathbf{r})$.

Definition 5.2.5. *The* ***parameter space of packings*** $\mathfrak{P}^\infty$ *is defined as the subset of* $\mathfrak{R}$ *given by* $\mathfrak{P}^\infty = \Theta^{-1}(\mathfrak{S}^\infty)$ *and its relative interior,* $\mathfrak{P}^\infty \cap (0,\infty)^k$*, is denoted* $\mathfrak{P}$*. While* $\mathfrak{P}^\infty$ *comprises the full set of radii vectors* $\mathbf{r}$ *giving hyperbolic complexes* $K(\mathbf{r})$ *which are packings,* $\mathfrak{P}$ *comprises those whose radii are finite.*

The angle sum map Θ carries $\mathfrak{P}^\infty$ onto $\mathfrak{S}^\infty$ and $\mathfrak{P}$ onto $\mathfrak{S} = \mathfrak{S}^\infty \cap (0,\infty)^k$. Note that since $\mathrm{carr}\,(P)$ lies in Ω, and the closure of Ω has been assumed to lie in $\mathbf{D}$, no boundary circles of P are horocycles. Thus the particular vector R of radii associated with P lies in $\mathfrak{P}$; we denote its image by

$$\Theta(R) = [\phi_1, \cdots, \phi_q \ ; \ 2\pi, \cdots, 2\pi] \tag{2}$$

and observe that the angles ϕ_j are strictly positive. The vector $\widetilde{R}$ associated with $\widetilde{P}$ lies in $\mathfrak{P}^\infty \backslash \mathfrak{P}$ and its image is

$$\Theta(\widetilde{R}) = [0, \cdots, 0 \ ; \ 2\pi, \cdots, 2\pi]. \tag{3}$$

We will find shortly that $\widetilde{R}$ lies in the boundary of $\mathfrak{P}$ in an appropriate sense. Indeed, our assumption that $\overline{\Omega} \subset \mathbf{D}$ has been made so that we could work in $\mathfrak{P}$, and is simply a convenience to avoid the extra bookkeeping which would be necessitated by infinite radii.

5.3. **Basic Results.** We must recall some of the known results regarding packings using our current terminology and notation. Place a partial ordering on vectors in radius space or angle space by writing $w \leq w'$ for vectors w, w' if their components satisfy $w_j \leq w'_j,\ 1 \leq j \leq k$.

Proposition 5.3.1 ([6]). *Let K be a DL-complex.*

(a). (Andreev's Theorem) There exists a unique vector $\widetilde{R}$ of radii for which $K(\widetilde{R})$ is a packing with $\widetilde{R}_j = \infty,\ 1 \leq j \leq q$; that is, having every boundary radius infinite.

(b). (Monotonicity) If $K(\mathbf{r})$ and $K(\mathbf{r}')$ are packings with $r_j \leq r'_j,\ 1 \leq j \leq q$, then $\mathbf{r} \leq \mathbf{r}'$. A single instance of equality $r_i = r'_i$ for $q < i \leq k$ implies $\mathbf{r} = \mathbf{r}'$.

(c). (Discrete Schwarz Lemma) If $K(\mathbf{r})$ is a packing, then $\mathbf{r} \leq \widetilde{R}$.

(d). (Discrete Pick Lemma) If $K(\mathbf{r})$ is a packing and v, w are vertices of K, then the hyperbolic distance in $K(\mathbf{r})$ from v to w is no greater than the hyperbolic distance in $K(\widetilde{R})$ from v to w.

Of course the hyperbolic complex $K(\widetilde{R})$ of part (a) is that associated with the Andreev packing $\widetilde{P}$ for K; its radii $\widetilde{R}$ are termed the **Andreev radii** for K. Part (b) says that in comparing two packings, the one with larger boundary radii will automatically have larger interior radii. Part (c) shows the extremal nature of $\widetilde{R}$; along with (d) it provides a discrete version of the hyperbolic contraction principle. Note this consequence of (b) and (c): If one DL-complex embeds as a proper subcomplex of a second, then each circle in the Andreev packing of the first will have larger hyperbolic radii than the corresponding circle in the Andreev packing of the second (i.e., smaller complex implies larger Andreev radii).

Another result from [6] which we need concerns "Dirichlet" type problems having to do with existence and uniqueness of packings with specified boundary radii. We include it, along with a parallel result for boundary angle sums.

Proposition 5.3.2. *Let K be a DL-complex.*

(a). Suppose boundary radii $r_j \in (0, \infty]$ are given, $j = 1, 2, \cdots, q$. Then there exists a unique vector $\hat{\mathbf{r}}$ so that $K(\hat{\mathbf{r}})$ is a packing and $\hat{r}_j = r_j,\ 1 \leq j \leq q$

(b). Suppose angles $\alpha_j \geq 0$ are given, $j = 1, 2, \cdots, q$, and assume there exists a packing $K(\mathbf{r}_0)$ whose boundary angle sums satisfy $\theta_j(\mathbf{r}_0) \geq \alpha_j,\ 1 \leq j \leq q$. Then there exists a unique vector $\hat{\mathbf{r}}$ so that $K(\hat{\mathbf{r}})$ is a packing and $\theta_j(\hat{\mathbf{r}}) = \alpha_j,\ 1 \leq j \leq q$.

Proof: Part (a) is a generalization of Andreev's Theorem, and the uniqueness follows from Proposition 5.3.1(b). The proof (see [6, Thm 3]) uses monotonicity and a version of the Perron method, which is associated with the classical Dirichlet problem. This proof of (b) is very similar:

Let $\mathfrak{F} \subseteq \mathfrak{R}$ denote the family of radius vectors $\mathbf{r}$ for which

$$\theta_j(\mathbf{r}) \geq \alpha_j,\ 1 \leq j \leq q, \quad \text{and} \quad \theta_i(\mathbf{r}) \geq 2\pi,\ q < i \leq k.$$

(In the terminology of [6], $K(\mathbf{r})$ is a "subpacking".) By hypothesis, $\mathbf{r}_0 \in \mathfrak{F}$, so $\mathfrak{F}$ is nonempty. We claim that the desired radius vector $\hat{\mathbf{r}}$ has components defined by

$$\hat{r}_j = \sup\{r_j : \mathbf{r} \in \mathfrak{F}\}.$$

Straightforward arguments (see [6, §5]) using the Monotonicity Lemma prove that $\mathfrak{F}$ is closed under least upper bounds, and the continuity of angle sums proves that $\hat{\mathbf{r}} \in \mathfrak{F}$.

Consider a vertex v_j, and suppose that $\theta_j(\hat{\mathbf{r}}) > \alpha_j$ if $j \leq q$ or that $\theta_j(\hat{\mathbf{r}}) > 2\pi$ if $q < j \leq k$. In either case, $\hat{r}_j$ is necessarily finite, and after it is incremented by a small amount, this inequality will persist. On the other hand, by the Monotonicity Lemma, such an increment in $\hat{r}_j$ can only increase other angle sums. Consequently, the incremented vector would be a vector in $\mathfrak{F}$ with j^{th} component greater than $\hat{r}_j$, contrary to the definition of the latter. Therefore,

$$\theta_j(\mathbf{r}) \leq \alpha_j, \ 1 \leq j \leq q, \quad \text{and} \quad \theta_i(\mathbf{r}) \leq 2\pi, \ q < i \leq k.$$

The opposite inequalities hold because $\hat{\mathbf{r}} \in \mathfrak{F}$. We conclude that $K(\hat{\mathbf{r}})$ is a packing and that it has precisely the desired boundary angle sums.

Uniqueness follows from area considerations. If F is the number of faces of K, the hyperbolic area of $K(\mathbf{r})$ can be found by applying the Area Rule and grouping the face angles according to their vertex:

$$\text{Area}\,(K(\mathbf{r})) = F\pi - \sum_{j=1}^{k} \theta_j(\mathbf{r}).$$

Suppose now that $\mathbf{r}$ were another vector with $\theta_j(\mathbf{r}) = \alpha_j = \theta_j(\hat{\mathbf{r}}), \ j = 1, 2, \cdots, k$. On the one hand, $\text{Area}\,(K(\mathbf{r})) = \text{Area}\,(K(\hat{\mathbf{r}}))$. On the other, $\mathbf{r} \in \mathfrak{F}$, so $\mathbf{r} \leq \hat{\mathbf{r}}$ by the definition of $\hat{\mathbf{r}}$. Strict inequality in one or more components along with the Monotonicity Lemma would imply $\text{Area}\,(K(\mathbf{r})) < \text{Area}\,(K(\hat{\mathbf{r}}))$. We conclude that $\mathbf{r} = \hat{\mathbf{r}}$, proving uniqueness. □

5.4. **The Path.** We are now in position to define the desired path from P to $\widetilde{P}$ within the space of packings and to establish its central properties. By the uniqueness given in part (b) above, $\Theta : \mathfrak{R} \longrightarrow \mathfrak{A}$ is injective. The components of Θ, as sums of expressions involving the Cosine Rule, are differentiable when all radii involved are finite, so the restriction of Θ to $\mathfrak{P}$ is a differentiable mapping of $\mathfrak{P}$ into the q-dimensional affine space $\mathfrak{S}$. In particular, $\mathfrak{P}$ is a differentiable q-dimensional submanifold of $(0, \infty)^k$.

Let $\lambda(t)$ be the line segment in $\mathfrak{S}^\infty$ given by

$$\lambda(t) = (1-t)\Theta(R) + t\Theta(\widetilde{R}) \ , \quad t \in [0, 1] \ .$$

In particular, by (2) and (3),

$$\lambda(t) = [(1-t)\phi_1, (1-t)\phi_2, \cdots, (1-t)\phi_q \ ; \ 2\pi, \cdots, 2\pi] \ , \quad t \in [0, 1] \ .$$

Since the ϕ_j are positive, $\lambda(t) \in \mathfrak{S}, \ t \in [0, 1)$, and its first q components (the boundary angle sums) are strictly decreasing in t. By Proposition 5.3.2(b), for each $t \in [0, 1)$

there exists a unique $\mathbf{r} = \mathbf{r}(t) \in \mathfrak{P}$ so that $\Theta(\mathbf{r}(t)) = \lambda(t)$. The differential associated with the curve λ in angle space is

$$d\lambda = [-\phi_1, \cdots, -\phi_q \ ; \ 0, \cdots, 0]\, dt \ ,$$

so the differential $d\mathbf{r}$ in radius space, if it exists, must satisfy

$$\left(\frac{\partial \Theta}{\partial \mathbf{r}}\right) \cdot d\mathbf{r}^{tr} = d\lambda^{tr}, \tag{4}$$

where $\left(\frac{\partial \Theta}{\partial \mathbf{r}}\right) = [\frac{\partial \theta_j}{\partial r_j}]$ denotes the $k \times k$ Jocobian matrix of Θ.

Proposition 5.4.1. *The curve* $\mathbf{r} = \Theta^{-1} \circ \lambda : [0,1) \longrightarrow \mathfrak{P}$ *is a simple and differentiable curve which starts at* R *and converges to* $\widetilde{R}$ *as* $t \uparrow 1$.

Proof: Differentiability would follow from the implicit function theorem, the differentiability of Θ, and the differentiability of λ. Rather than pursue that line, however, we explicitly solve (4) for $d\mathbf{r}$ in Section 7.

The behavior as t approaches 1 also depends on our solution of (4), for it turns out that $\mathbf{r}(t)$ is strictly increasing in t. Assuming this for the moment, consider the angle sum $\theta_j(\mathbf{r}(t))$ at a boundary vertex v_j. Suppose the triangle T of Figure 5 represents one of the faces to which v_j belongs, with $v = v_j$ and u, w two neighbors. By the Monotonicity Lemma, the angle ψ at v is increasing in the s-radii u and w. With v, u, w all increasing, therefore, it is clear that ψ can go to zero only if v goes to infinity. Since the boundary angle sums along λ go to zero as $t \uparrow 1$, the boundary radii $r_j(t),\ 1 \leq j \leq q$, must go to infinity, their Andreev values. It is then an easy argument using Proposition 5.3.1 to show that the interior radii also converge to their Andreev values. Thus, $\mathbf{r}(t) \to \widetilde{R}$ as $t \uparrow 1$, so we can define $\mathbf{r}(1) = \widetilde{R}$. This completes the proof, modulo the computation of $d\mathbf{r}$ in §7. □

Summary 5.4.2. *The map* $t \mapsto \mathbf{r}(t)$ *is a continuous map of* $[0,1]$ *into* $\mathfrak{P}^\infty$ *and will be referred to simply as the* ***path*** *in the sequel. The path lies in* $\mathfrak{P}$ *and is differentiable for* $t \in [0,1)$, *while* $\mathbf{r}(1) = \widetilde{R}$. *The associated path of hyperbolic complexes* $K(\mathbf{r}(t))$ *is a smoothly parameterized path of packings, starting with the packing* $K(\mathbf{r}(0)) = K(R)$ *corresponding to* P *and ending with the packing* $K(\mathbf{r}(1)) = K(\widetilde{R})$ *corresponding to* $\widetilde{P}$.

6. The Markov Model

6.1. **Introduction.** We continue studies related to the fixed circle packing P with complex K. In this section we develop probabilistic models which can be associated with packings $K(\mathbf{r}),\ \mathbf{r} \in \mathfrak{P}$. For each $K(\mathbf{r})$, there are actually three Markov processes — a basic model and two "absorbing" modifications. We compute explicit transition probabilities and affiliated conductances and explain how to manipulate distributions of curvature. (The quantities under study are functions of $\mathbf{r}$, but we suppress that dependence in our notation.) In a final subsection, we introduce some of the generic

probabilistic paraphernalia we will need for working with random walks: escape probabilities, stopping times, effective conductances, discrete harmonic functions, and so forth.

6.2. **Markov Processes.** We will be working with discrete Markov processes, also known as Markov chains or random walks. A standard reference is [28], though we make direct use of several ideas presented in Doyle and Snell [11] and highly recommend this beautiful little book to the reader.

In a discrete Markov process, one has a collection of **states** and a collection of **transition probabilities** between states. Time is treated as discrete, and one is interested in the distribution of some quantity (in our case, curvature) among the states over time. There are two viewpoints one can take: (1). The transition probabilities may be placed in a **transition matrix** T; this matrix operates on row vectors W which represent the distribution of curvature among the states at a given time. For instance, the row vector $W \cdot T$ gives the distribution after the next time step, $W \cdot T^2$ the distribution after a second time step, and so forth. (2). The more intuitive and colorful alternative involves random walkers. A random walker represents a quantum of curvature, much like an electron represents a quantum of electrical current; if the random walker starts in state i, say, then it moves to state j with probability p_{ij} at the first time step, to state k with probability p_{jk} at the next time step, and so on. The probabilities of various events are then reflected in the average behavior of large numbers of such random walkers.

Both viewpoints will be useful. The quantity we model is a form of differential curvature distributed among the vertices of K. Starting with an initial distribution on the boundary vertices, we are interested in its movement about the complex over time. As we shall see, the specifics of the model depend on the particular radius vector $\mathbf{r}$, which we take to lie in $\mathfrak{P}$. Initially, we define an ergodic process $\mathfrak{M}$. The processes of interest, however, are modifications in which certain states become absorbing — walkers reaching those states never leave.

6.3. **The Graph G.** Ideally, the state space for our Markov processes would be the set of vertices of K. However, each of the k vertices serves a dual role as both absorbing and non-absorbing. Our device for handling this involves introducing twin nodes:

Definition 6.3.1. *Define the graph G consisting of the one-skeleton of K along with a set of k additional nodes, each attached via an edge to precisely one node of K. No confusion should result if we use the notation v_j both for a vertex of K and for the corresponding node of G; this will be called a* ***standard*** *node. The node attached to v_j will be denoted v_j' and termed a* ***twin*** *node. In all vector and matrix quantities associated with the nodes, our ordering places the k twin nodes first, followed by the k standard nodes; thus we have the state space $\{v_1', \cdots, v_k', v_1, \cdots, v_k\}$.*

We will be defining three closely related discrete Markov processes on G by giving the transition probabilities for the edges of G. (The edges have been included in the

state space G only to suggest our electrical analogy.) The basic underlying process is $\mathfrak{M}$; the processes of interest are $\mathfrak{M}^a$, obtained from $\mathfrak{M}$ by making the twin nodes absorbing, and $\mathfrak{M}^b$, obtained from $\mathfrak{M}^a$ by also making the standard boundary nodes absorbing. These modifications simply involve changes in certain of the transition probabilities.

6.4. **The Basic Model.** Transition probabilities are of two types: between standard nodes and between a standard node and its twin. We will give the definitions and notation first and then verify that they define an ergodic random walk. Here, A_i represents the hyperbolic area of the faces of $K(\mathbf{r})$ in the star of the vertex v_i and θ_i represents the angle sum at v_i, as defined in §5.2.2. The probabilities are expressed in terms of both hyperbolic radii and s-radii.

Definition 6.4.1. *The* ***transition probability*** *from standard node v_i to standard node v_j is*

$$p_{ij} = -(\frac{\partial\theta_j}{\partial r_i})(\frac{\partial\theta_i}{\partial r_i})^{-1} = -(\frac{\partial\theta_j}{\partial v_i})(\frac{\partial\theta_i}{\partial v_i})^{-1}.$$

The transition probability from standard node v_i to the twin node v_i', termed a ***leakage probability****, is*

$$p_{ii'} = -(\frac{\partial A_i}{\partial r_i})(\frac{\partial\theta_i}{\partial r_i})^{-1} = -(\frac{\partial A_i}{\partial v_i})(\frac{\partial\theta_i}{\partial v_i})^{-1}.$$

The transition probability from v_i' to v_i is defined to be $p_{i'i} = 1$ (recall that v_i is the only neighbor of v_i').

We have seen in Section 4 that these derivatives exist, and by Lemma 4.4.1(i) and the fact that the radii in $\mathbf{r}$ are finite, the derivative appearing in the denominators is nonzero, so these quantities are well defined. Verification that they are probabilities requires some hyperbolic geometry.

Consider the star of faces for a vertex v_i in $K(\mathbf{r})$. Suppose v_i has n neighbors $v_1, \cdots, v_n$, and for each j, $1 \leq j \leq n$, let α_j be the sum of the angles at v_j in the (one or two) faces to which it belongs in the star of v_i. Recall that $\theta_i = \theta_i(\mathbf{r})$ denotes the sum of angles at v_i. By the area formula for hyperbolic triangles, with rearrangement and grouping of angles, we may express the area A_i of the star of v_i as

$$A_i = n\pi - \theta_i - \sum_{j=1}^{n} \alpha_j.$$

Computing the partial derivative with respect to r_i, while recognizing that $\frac{\partial \theta_j}{\partial r_i} = \frac{\partial \alpha_j}{\partial r_i}, j = 1, \cdots, n$, yields the identity

$$\frac{\partial \theta_i}{\partial r_i} = -\frac{\partial A_i}{\partial r_i} - \sum_{j=1}^{n} \frac{\partial \theta_j}{\partial r_i}. \tag{5}$$

Multiplying both sides of (5) by $(\frac{\partial \theta_i}{\partial r_i})^{-1}$ gives

$$1 = p_{ii'} + \sum_{j=1}^{n} p_{ij}. \tag{6}$$

Of course, $p_{ij} = 0$ if v_i and v_j are not neighbors; while by the Monotonicity Lemma, $p_{ij} > 0$ if v_i and v_j are neighbors, and $p_{ii'} > 0$. The equality in (6) therefore justifies the probabilistic interpretation. Moreover, because K is connected and has k nodes, it is not difficult to see that for any $1 \leq j \leq k$, a random walker starting at, say, v_1 will have some positive probability of being at v_j after k steps. This implies that the random walk is **aperiodic**. Therefore

Definition 6.4.2. *The transition probabilities defined in §6.4.1 determine an ergodic Markov process $\mathfrak{M}$ on the graph G.*

The identity (5) is what motivates the choice of transition probabilities and is of fundamental importance in our development. It expresses the fact that any change in the angle sum θ_i (caused by a change in r_i) is exactly matched by changes in the area of the star of v_i and changes in the angle sums of neighboring vertices. The reader should note that the transition and leakage probabilities are functions of the radius vector $\mathbf{r}$; actual changes in radii would alter the transition probabilities of the model, so all "changes" which we discuss are to be interpreted in the differential sense.

6.5. **Conductances.** It is interesting, and in any case required for later work, to develop the transition probabilities for $\mathfrak{M}$ from another standpoint; namely, by defining what are known as conductances of the edges of G. For notation we refer to the circle configuration of Figure 5, consisting of the end nodes v, w of an edge and their common neighbors u, a. Recall that these symbols also denote the s-radii of the corresponding nodes; in particular, they all exceed 1. The auxiliary functions g and h are defined in §4.3.2.

Definition 6.5.1. *The **conductances** of edges of G are defined as follows:*
For the edge (v, w) of Figure 5,

$$\begin{aligned} \mathcal{C}_{vw} = \mathcal{C}_{wv} &= (g_3(w,u,v) + g_3(w,a,v))\sqrt{v}(v-1) = h(w,u,a,v)\sqrt{v}(v-1) \\ &= \frac{\sqrt{vw(v-1)(w-1)}}{(vw-1)}\Big[\sqrt{\frac{u-1}{uvw-1}} + \sqrt{\frac{a-1}{avw-1}}\Big]. \end{aligned}$$

(In case the nodes v and w have only one common neighbor, say u, the radical involving a is omitted.)

For the edge (v, v') between a standard node and its twin,

$$\mathcal{C}_{vv'} = \mathcal{C}_{v'v} = \Big[\sum_{(v,u,w)} (-g_1(v,u,w) - g_2(u,v,w) - g_3(w,u,v)) \Big] \sqrt{v}(v-1)$$

$$= \sum_{(v,u,w)} \frac{\sqrt{(v-1)(u-1)(w-1)}}{(vw-1)(uv-1)\sqrt{uvw-1}} \big[(uv^2w-1) - \sqrt{vw}(uv-1) - \sqrt{uv}(vw-1) \big],$$

where the sum is over all triples (v, u, w) forming faces in the star of v.

The total of the conductances for all edges emanating from node v is the ***node conductance*** *and is denoted $\mathcal{C}_v$, and the* ***total conductance*** *of G is the sum of all edge conductances, $\mathcal{C} = \sum_v \mathcal{C}_v$. (We will also use the notations $\mathcal{C}_{ij}$ and $\mathcal{C}_j$ for edge and node conductances when the vertices are indexed.)*

We can represent these conductances in more familiar terms: First, note that by the Cosine Rule, the auxiliary function $g(x, y, z)$ gives the angle at x in the hyperbolic triangle formed by circles with s-radii x, y, z. Let us return to the setting immediately following §6.4.1, with a vertex v_i and its neighbors $v_1, \cdots, v_n$. By considering the edge from v_i to one of the v_j, and taking care with the order of the arguments, we see that

$$\frac{\mathcal{C}_{ij}}{\sqrt{v_i}(v_i - 1)} = \frac{\partial \alpha_j}{\partial v_i} = \frac{\partial \theta_j}{\partial v_i}.$$

Next, consider a face (v_i, v_j, v_l); by the Area Rule, its hyperbolic area is $\pi - g(v_i, v_l, v_j) - g(v_l, v_j, v_i) - g(v_j, v_i, v_l)$. Differentiating and summing over all faces in the star of v_i, we see that

$$\frac{\mathcal{C}_{ii'}}{\sqrt{v_i}(v_i - 1)} = \frac{\partial A_i}{\partial v_i}.$$

Thus, the conductances are closely related to the geometric quantities we have been studying. If we multiply the fundamental identity

$$\frac{\partial A_i}{\partial v_i} + \sum_{j=1}^{n} \frac{\partial \theta_j}{\partial v_i} = -\frac{\partial \theta_i}{\partial v_i}$$

by $\sqrt{v_i}(v_i - 1)$, we see that the node conductances satisfy

$$\frac{\mathcal{C}_i}{\sqrt{v_i}(v_i - 1)} = -\left(\frac{\partial \theta_i}{\partial v_i}\right).$$

Putting these expressions together with the definitions of the transition probabilities, we have

$$
\begin{aligned}
p_{ij} &= -\left(\frac{\partial\theta_j}{\partial v_i}\right)\left(\frac{\partial\theta_i}{\partial v_i}\right)^{-1} = -\left(\frac{\partial\theta_j}{\partial v_i}\right)\left(\sqrt{v_i}(v_i-1)\right)\left(\frac{\partial\theta_i}{\partial v_i}\right)^{-1}\left(\frac{1}{\sqrt{v_i}(v_i-1)}\right) = \frac{\mathcal{C}_{ij}}{\mathcal{C}_i}\ , \\
p_{ii'} &= -\left(\frac{\partial A_i}{\partial v_i}\right)\left(\frac{\partial\theta_i}{\partial v_i}\right)^{-1} = -\left(\frac{\partial A_i}{\partial v_i}\right)\left(\sqrt{v_i}(v_i-1)\right)\left(\frac{\partial\theta_i}{\partial v_i}\right)^{-1}\left(\frac{1}{\sqrt{v_i}(v_i-1)}\right) = \frac{\mathcal{C}_{ii'}}{\mathcal{C}_i}\ , \\
p_{i'i} &= \frac{\mathcal{C}_{i'i}}{\mathcal{C}_{i'}} = \frac{\mathcal{C}_{ii'}}{\mathcal{C}_{i'}} = \frac{\mathcal{C}_{i'}}{\mathcal{C}_{i'}} = 1\ .
\end{aligned}
\tag{7}
$$

That is, one can determine all the transition probabilities of the Markov process $\mathfrak{M}$ from the conductances alone.

The use of conductances to define the transition probabilities is standard in the study of Markov chains; indeed, the existence of such conductances characterizes what are known as **reversible** random walks. The important identity

$$p_{ij}\mathcal{C}_i = p_{ji}\mathcal{C}_j \tag{8}$$

follows from the fact that $\mathcal{C}_{ij} = \mathcal{C}_{ji}$.

6.6. **Two Absorbing Models.** The differentials of angle sums may be thought of informally as **curvature**, and it is the movement of this curvature among the vertices of K which our random walk on G models: curvature driven away from one node is distributed to neighboring nodes according to the transition probabilities; it is then distributed to their neighbors; and so forth and so on. However, that portion of curvature going to twin nodes represents angle converting to area — it no longer affects any neighbors and should be removed from the process. We model this as leakage to the twin nodes, and force it to remain there by declaring all twin nodes to be absorbing states.

Definition 6.6.1. *Modify the transition probabilities of* $\mathfrak{M}$ *by declaring* $p_{i'i'} = 1$, $p_{i'i} = 0$, $i = 1, \cdots, k$. *Thus, a random walker visiting a twin node* v_i' *will never leave. The resulting process is denoted by* $\mathfrak{M}^a$ *and is termed an absorbing random walk.*

It is convenient for our use of $\mathfrak{M}^a$ to represent it *via* its transition matrix T; this is the $2k \times 2k$ matrix of transition probabilities whose i, j entry is the probability that a random walker in state i will be in state j after one time step. Because of the convention we made regarding the ordering of states, we may write T in $k \times k$ block form as

$$T = \begin{bmatrix} I & 0 \\ L & Q \end{bmatrix}\ .$$

The $k \times k$ identity matrix I occurring in the upper left position and the $k \times k$ zero matrix in the upper right reflect the fact that the k twin nodes are absorbing. Indeed, the only way to reach an absorbing node v_i' is *via* its standard twin v_i, so the lower left

$k \times k$ block is the diagonal matrix $L = [p_{ii'}]$ of leakage probabilities. The lower right $k \times k$ block is the matrix of transition probabilities between standard nodes

$$Q = \begin{bmatrix} 0 & p_{12} & \dots & p_{1k} \\ p_{21} & 0 & \dots & p_{2k} \\ \vdots & \vdots & \ddots & \vdots \\ p_{k1} & p_{k2} & \dots & 0 \end{bmatrix}.$$

Let $T^\infty = \lim_n T^n$. Because the diagonal entries of L are strictly positive, the row sums of Q are strictly less than 1. It follows that $(I - Q)^{-1} = I + Q + Q^2 + \cdots$ converges, and that T^∞ has the $k \times k$ block form

$$T^\infty = \begin{bmatrix} I & 0 \\ B & 0 \end{bmatrix},$$

where B is the $k \times k$ matrix $B = (I - Q)^{-1} \cdot L$.

The Markov process works in the following way: Given an initial distribution of curvatures on the state space, represented as a $2k$-row vector, multiplication on the right by T gives the distribution after one time step, multiplication on the right by T again gives the distribution after two steps, and so forth. Multiplying the original distribution on the right by T^∞ gives the final distribution of curvature. Note that every random walker eventually reaches and remains at some twin node; so the process dies out over infinitely many steps, leaving the curvature entirely with the twin nodes. Indeed, an entry b_{ij} of B may be interpreted as the probability that a random walker (quantum of curvature) starting at standard node v_i will eventually be absorbed at the twin node v_j'.

Since it is the curvature on the standard nodes which drives the process, an alternate way to describe the action involves k-row vectors: If W represents an initial distribution of curvature among the standard nodes, then $W \cdot L$ represents the amounts absorbed by the twin nodes during one step (that is, its i^{th} entry is the amount of curvature absorbed by v_i') and $W \cdot Q$ represents the new distribution of curvature on the standard nodes after one step. In general, $W \cdot Q^{n-1} \cdot L$ represents the additional amounts absorbed by the twin nodes during the n^{th} step and $W \cdot Q^n$ gives the distribution of curvature after the n^{th} step. Since all curvature is eventually absorbed by the twin nodes, the vector

$$W \cdot (I + Q + Q^2 + \cdots) \cdot L = W \cdot (I - Q)^{-1} \cdot L$$

represents the final distribution of absorbed curvature among the twin nodes at the end of the process. Note that

$$W \cdot (I - Q)^{-1}$$

represents the total curvature visiting the standard nodes during the life of the process.

Our third Markov process is obtained from $\mathfrak{M}^a$ by making the standard boundary nodes of G absorbing.

Definition 6.6.2. *Modify the transition probabilities of $\mathfrak{M}^a$ by declaring $p_{ij} = 0$ and $p_{ii} = 1$ for all boundary nodes v_i, $i = 1, \cdots, q$. That is, a random walker visiting a boundary node will be absorbed there. The resulting process is denoted $\mathfrak{M}^b$.*

The other transition probabilities from $\mathfrak{M}^a$ remain unchanged — in particular, the twin nodes continue to be absorbing. (The reader should be cautioned that absorbing states are often called "boundary" states in the literature on random walks. For us, however, "boundary" is used to refer to those standard nodes of G associated with the topological boundary of K.)

6.7. **Preliminaries on Random Walks.** In the sequel we will be studying various Markov processes from the standpoint of random walkers rather than distributions, and we require some few additional preliminaries. Our statements are for generic random walks, though we use G for the graph and $\mathfrak{M}$ for the Markov process.

Let $\mathfrak{X}$ denote the space of sequences $\omega = \{\omega_0, \omega_1, \cdots\}$ of nodes of G; each sequence is termed a **sample path** and represents the path of a random walker on G. In an entirely standard way, a σ-algebra $\mathfrak{F}$ is generated by the cylinder sets $\{\omega : \omega_i = u_i, i = 0, 1, \cdots, n\}$ for all integers $n \geq 0$, nodes $u_0, \cdots, u_n \in G$. **Random variables** are simply $\mathfrak{F}$-measurable functions on $\mathfrak{X}$. For instance, we will use $\mathbf{X}_n$ to denote the random variable defined by $\mathbf{X}_n(\omega) = \omega_n$; that is, $\mathbf{X}_n$ gives the location of the random walker at the n^{th} time step.

The random walk starting at a non-absorbing node $v \in G$ may now be represented *via* a **probability measure** $\mathbf{P}_v$. Thus $\mathbf{P}_v[X_0 = v] = 1$, and the measure is entirely determined by this along with the transition probabilities of the process $\mathfrak{M}$. In particular, the conditional probability that the random walker is at w on the $(n+1)^{\text{st}}$ step, given that it is at v on the n^{th} step, is

$$\mathbf{P}_v[\mathbf{X}_{n+1} = w \mid \mathbf{X}_n = v] = p_{vw}.$$

Among other things, one can readily check that

$$\mathbf{P}_v[\mathbf{X}_n = y \mid \mathbf{X}_m = w] = \mathbf{P}_w[\mathbf{X}_{n-m} = y],\ 0 \leq m < n,\ y \in G.$$

(As is common practice, reference to the sample paths is suppressed in the notation.)

Given a real random variable f on $\mathfrak{X}$, the **expectation** of f for the random walk starting at v is defined by

$$\mathbf{E}_v[f] = \int_{\mathfrak{X}} f(\omega)\, d\mathbf{P}_v(\omega),$$

assuming this integral converges. A **stopping time** τ is a random variable taking values in $\{1, 2, \cdots\} \cup \{\infty\}$ which depends only on the past of a random walk; that is, the event $[\tau = n]$ is independent of $\mathbf{X}_{n+1}, \mathbf{X}_{n+2}, \cdots$. The stopping times we will use are called **hitting times**, and involve encounters with various sets. For example, given $S \subset G$, the first hitting time for S is $\tau = \min\{n > 0 : \mathbf{X}_n \in S\}$. More generally, if τ is a stopping time, then the stopping time $\tau_1 = \min\{n > \tau : \mathbf{X}_n \in S\}$ gives the first hitting time after τ.

Later we will be interested in nodes "deep" inside a graph, in the sense that it is difficult for random walkers starting there to reach some designated set (usually described as a "boundary").

Definition 6.7.1. *Given a set $S \subset G$ and $v \in G \backslash S$, define p_{esc} as the probability that a random walker starting at v will encounter S before returning to v. Then p_{esc} is called the* ***escape probability*** *from v to S.*

As long as there is positive probability of hitting S, p_{esc} will be positive. A small value for p_{esc} suggests that the set S is far from v, in that random walkers are unlikely to reach it without repeated attempts. All our random walks are reversible, and in this setting a related concept is that of the **effective conductance**, $\mathcal{C}_{\text{EFF}}$ from v to S. (In an electrical circuit, this reflects the conductance that a single wire connecting v and S would need to account for the same current flow as does G.) If $\mathcal{C}_v$ denotes the node conductance at v (the sum of the conductances of edges leaving v), then

$$p_{\text{esc}} = \frac{\mathcal{C}_{\text{EFF}}}{\mathcal{C}_v}.$$

The probabilistic interpretation of a beautiful result by J. W. S. Rayleigh regarding electrical circuits states that effective conductance is monotone in the individual edge conductances, [11, Chp. 4].

Lemma 6.7.2 (Rayleigh's Monotonicity Law)**.** *Let $S \subset G$ and $v \in G \backslash S$. Suppose $\mathbf{C}$ and $\mathbf{C}'$ are collections of conductances for the edges of G satisfying $\mathbf{C} \leq \mathbf{C}'$; that is, each conductance in the former is less than or equal to the corresponding conductance in the latter. Then their effective conductances from v to S satisfy $\mathcal{C}_{EFF} \leq \mathcal{C}'_{EFF}$.*

The **simple** random walk on a graph G is one in which, at each step, the random walker has equal probability of moving along any edge from its current node. This is the reversible random walk which results if all edges are given identical conductances.

The connections between Brownian motion and potential theory are well known, and there is a parallel connection between random walks and discrete potential theory. We continue to use $\mathfrak{M}$ and G in a generic sense.

Definition 6.7.3. *A (discrete) harmonic function for a Markov process $\mathfrak{M}$ on the graph G is a real function h on G satisfying the* ***mean value property*** *given by*

$$h(v) = \sum_{w \in G} h(w) p_{vw}, \ v \in G.$$

Equivalently, if T is the transition matrix for $\mathfrak{M}$ and h is represented as a column vector, then $T \cdot h = h$.

The discrete mean value property (analogue of the classical integral mean value property for a circle) may be restated as

$$\mathbf{E}_v[h(\mathbf{X}_1)] = \sum_{w \in G} h(w) \mathbf{P}_v[\mathbf{X}_1 = w] = \sum_{w \in G} h(w) p_{vw} = h(v), \ \forall v \in G.$$

It is not difficult from this to show that for h harmonic,

$$\mathbf{E}_v[h(\mathbf{X}_n)] = h(v),\ \forall v \in G,\ n = 0, 1, \cdots .$$

An important generalization of this involves random times:

Lemma 6.7.4. *If τ is a stopping time for $\mathfrak{M}$ with $\mathbf{P}_v[\tau < \infty] = 1$ and if h is a discrete harmonic function for $\mathfrak{M}$, then*

$$\mathbf{E}_v[h(\mathbf{X}_\tau)] = h(v),\ \forall v \in G.$$

7. Computations from the Model

7.1. **Introduction.** We apply the Markov model specifically to the intermediate packings on the path from P to $\widetilde{P}$ which we defined in Section 5. In particular, assuming $t \in [0, 1)$ is fixed, we find ourselves at the point $\mathbf{r}(t) \in \mathfrak{P}$ in parameter space and must compute, among other things, the direction $d\mathbf{r}$ to move in order to remain on the path. In theory, one can compute $d\mathbf{r}$ from (4), since all the quantities involved are known specifically. However, crucial information is then obscured; in particular, movement of the conserved quantity, curvature, is confounded with the radii adjustments which drive it. The probabilistic methods allow us to separate these; in addition to solving for $d\mathbf{r}$, we can obtain important "visitation" information on the movement of curvature.

7.2. **Computation of $d\mathbf{r}$.** We employ the Markov model from the viewpoint of distributions and using the general prescriptions in Section 6.6. Given an initial distribution of curvature among the nodes of G, the model presents us with its final distribution after leaking to ground. This should all be thought of as information in "angle space" which, after an additional step, can be converted to "radius space".

Since the path $\mathbf{r}$ is identified, *via* the angle sum map Θ, with the path λ, the initial distribution of curvature (among the standard nodes) which we choose to study is

$$d\lambda = [-\phi_1, \cdots, -\phi_q\ ;\ 0, \cdots, 0]\, dt\ .$$

(The fact that the entries of $d\lambda$ are nonpositive will cause no mathematical difficulty and is consistent with our descriptions of this model: we want to change $\mathbf{r}$ so that the boundary angle sums decrease.) The amount of curvature visiting the standard nodes during the life of this process is an important quantity, and we will give it a name for later use. The reader may refer to §5 to recall our notations.

Definition 7.2.1. *The **visitation distribution** V is the vector defined by*

$$V = \frac{d\lambda}{dt} \cdot (I - Q)^{-1} = [V_1, \cdots, V_k].$$

Each component V_j is nonpositive and respresents the total curvature visiting the standard node v_j during the life of the process $\mathfrak{M}^a$, assuming the initial distribution of curvature is given by $d\lambda$.

The Markov process *per se* is concerned with differentials of angle sums; the connection with radii is provided by the $k \times k$ diagonal matrix $D = [\frac{\partial \theta_j}{\partial r_j}]$. If a quantity of curvature arriving at a node v_j is denoted $d\theta_j$, then its arrival requires an adjustment $dr_j = (\frac{\partial \theta_j}{\partial r_j})^{-1} d\theta_j$ in the radius at v_j to disperse it to area and the neighbors; and these adjustments accumulate with the successive steps of the process. The total accumulation of adjustments can be determined from the visitation distribution, and we have the

Proposition 7.2.2. *The vector of radius differentials associated with the path* $\mathbf{r}(t)$ *is given by* $d\mathbf{r} = d\lambda \cdot (I - Q)^{-1} \cdot D^{-1} = (V \cdot D^{-1})\, dt$. *That is,*

$$dr_j = V_j \big(\frac{\partial \theta_j}{\partial r_j}\big)^{-1} dt, \quad j = 1, 2, \cdots, k. \tag{9}$$

In particular, the components of $d\mathbf{r}$ *are positive, so along the path* $\mathbf{r}(t)\,,\ t \in [0, 1]$, *all radii are strictly increasing.*

Note that the existence and monotonicity here are what we needed in the proof of Proposition 5.4.1 earlier; positivity of $d\mathbf{r}$ is a strengthening at the differential level of the strict monotonicity in the Monotonicity Lemma 4.4.2.

Proof: We must verify that the vector $d\mathbf{r}$ satisfies equation (4); namely,

$$(\frac{\partial \Theta}{\partial r}) \cdot d\mathbf{r}^{\mathrm{t}} = d\lambda^{\mathrm{t}}.$$

First, compute $(\frac{\partial \Theta}{\partial r}) \cdot D^{-1}$.

$$(\frac{\partial \Theta}{\partial r}) \cdot D^{-1} = \begin{bmatrix} \frac{\partial \theta_1}{\partial r_1} & \frac{\partial \theta_1}{\partial r_2} & \cdots & \frac{\partial \theta_1}{\partial r_k} \\ \frac{\partial \theta_2}{\partial r_1} & \frac{\partial \theta_2}{\partial r_2} & \cdots & \frac{\partial \theta_2}{\partial r_k} \\ \vdots & \vdots & \ddots & \vdots \\ \frac{\partial \theta_k}{\partial r_1} & \cdots & \cdots & \frac{\partial \theta_k}{\partial r_k} \end{bmatrix} \cdot \begin{bmatrix} (\frac{\partial \theta_1}{\partial r_1})^{-1} & & & \\ & \ddots & & \\ & & & (\frac{\partial \theta_k}{\partial r_k})^{-1} \end{bmatrix}$$

$$= \begin{bmatrix} 1 & \frac{\partial \theta_1}{\partial r_2}(\frac{\partial \theta_2}{\partial r_2})^{-1} & \cdots & \frac{\partial \theta_1}{\partial r_k}(\frac{\partial \theta_k}{\partial r_k})^{-1} \\ \frac{\partial \theta_2}{\partial r_1}(\frac{\partial \theta_1}{\partial r_1})^{-1} & 1 & \cdots & \frac{\partial \theta_2}{\partial r_k}(\frac{\partial \theta_k}{\partial r_k})^{-1} \\ \vdots & \vdots & \ddots & \vdots \\ \frac{\partial \theta_k}{\partial r_1}(\frac{\partial \theta_1}{\partial r_1})^{-1} & \cdots & \cdots & 1 \end{bmatrix}$$

$$= \begin{bmatrix} 1 & -p_{21} & \cdots & -p_{k1} \\ -p_{12} & 1 & \cdots & -p_{k2} \\ \vdots & \vdots & \ddots & \vdots \\ -p_{1k} & -p_{2k} & \cdots & 1 \end{bmatrix}$$

$$= (I - Q)^{t}.$$

Plugging in our proposed $d\mathbf{r}$ from (9), we have

$$(\frac{\partial \Theta}{\partial r}) \cdot d\mathbf{r}^{t} = (\frac{\partial \Theta}{\partial r}) \cdot D^{-1} \cdot ((I - Q)^{t})^{-1} \cdot d\lambda^{t} = (I - Q)^{t}((I - Q)^{t})^{-1} \cdot d\lambda^{t} = d\lambda^{t},$$

verifying that $d\mathbf{r}$ satisfies equation (4).

Regarding positivity, recall our assumption that the boundary circles of P have finite radius. This implies that its boundary angle sums ϕ_j , $j = 1, \cdots, q$, are positive, and hence that the initial distribution $d\lambda$ is negative in its first q entries. One can, in addition, verify that the visitation distribution has negative entries using these facts about the matrix Q: (i) if v_i and v_j are interior neighbors, then $p_{ij} > 0$; (ii) every boundary vertex of K has an interior neighbor; and (iii) every pair of interior vertices can be connected by a chain of edges having only interior endpoints. Since D also has

entries which are negative, we conclude that the components of $d\mathbf{r} = (V \cdot D^{-1})\, dt$ are positive. □

7.3. **The Weighted Visitation Function.** An important function on the state space G is derived from the visitation distribution:

Definition 7.3.1. *The* ***weighted visitation function*** U *is the nonnegative function defined on the nodes of* G *by*

$$U(v) = \begin{cases} -V_j/\mathcal{C}_j, & \text{when } v \text{ is a standard node } v_j \\ 0, & \text{when } v \text{ is a twin node } v_j', \end{cases}$$

where the V_j *are the components of the visitation distribution* V *and the* $\mathcal{C}_j$ *are the node conductances associated with* $\mathfrak{M}$.

This function U is in some sense a dual object to V, and reflects the evenness with which curvature distributes itself. It satisfies the mean value property at standard interior nodes of G, but not at the boundary nodes where the original charge was placed. This is the reason for our introduction of the absorbing process $\mathfrak{M}^b$.

Lemma 7.3.2. *The weighted visitation function* U *is a nonnegative harmonic function for* $\mathfrak{M}^b$.

Proof: Given a k-vector W, we write $[W]_p$ for the p-vector consisting of its last p coordinates. The visitation distribution V is defined as $\dfrac{d\lambda}{dt} \cdot (I - Q)^{-1}$. Since the last p components of $\dfrac{d\lambda}{dt}$ are zero, we have

$$[V]_p = [\frac{d\lambda}{dt} \cdot (I + Q + Q^2 + \cdots)]_p = [\frac{d\lambda}{dt} \cdot (Q + Q^2 + \cdots)]_p = [V \cdot Q]_p.$$

(These last coordinates are those associated with interior nodes.) This equality implies by direct verification using the matrix Q that V satisfies

$$V_j = \sum_i V_i p_{ij} \ , \quad q+1 \le j \le k \, .$$

Note the subscript order; this is **not** the mean value property. However, we have the identity (8), $p_{ij} = p_{ji}\mathcal{C}_j/\mathcal{C}_i$. Substituting in the expression above and dividing both sides by $-\mathcal{C}_j$ gives

$$-\frac{V_j}{\mathcal{C}_j} = \sum_i (-\frac{V_i}{\mathcal{C}_i})\, p_{ji} \, , \quad q < j \le k \, ,$$

implying

$$U(v_j) = \sum_i U(v_i) p_{ji} \, , \quad q < j \le k \, .$$

This is the mean value property for U at standard interior nodes of G; the mean value property at absorbing nodes v is trivial since $p_{vv} = 1$. Therefore, U is harmonic for $\mathfrak{M}^b$. □

7.4. **Remark.** The initial distribution $d\lambda$ which we studied here arises because of its association with the path $\mathbf{r}$ in radius space. But we could equally well apply our model to other initial distributions among the boundary nodes. For example, suppose $\mathbf{r}_0 \in \mathfrak{P}$ and $\Theta(\mathbf{r}_0) \in \mathfrak{S}$ (see §5.2 for definitions). A vector in the tangent space of $\mathfrak{S}$ has the form $[d\theta_1, \cdots, d\theta_q \ ; \ 0, \cdots, 0]$, its first q coordinates representing differentials in the boundary angle sums. If we treat this as an initial distribution in the Markov model for $K(\mathbf{r}_0)$, then our computations provide the corresponding tangent vector to $\mathfrak{P}$ at $\mathbf{r}_0$; that is, the requisite differential changes in radii (boundary and interior). Note that the q degrees of freedom represented by the boundary angle sums along with Proposition 5.3.2(b) account for the q-dimensionality of $\mathfrak{P}$.

Putting this generality aside, however, the packings we will be using are associated with the path $\mathbf{r}(t)$. The processes $\mathfrak{M}, \mathfrak{M}^a$, and $\mathfrak{M}^b$ and the various related objects — the transition probabilities, matrices, conductances, visitation distributions, and so forth — are functions of t, though this dependence is not part of the notations.

8. Geometric Hypotheses and Estimates

8.1. **Introduction.** Our work so far applies to quite general circle packings. Here we inject the necessary geometric hypotheses and establish preliminary estimates.

8.2. **Notation and Hypotheses.** Recall that $E \subset \Omega$ is a fixed compact Jordan region. We require a buffer around E, so choose compact Jordan regions E_1 and E_2 with $E \subset E_1 \subset E_2 \subset \Omega$ so that

$$\min\{\text{dist}(E, E_1^c), \text{dist}(E_1, E_2^c)\} > \eta > 0.$$

These sets and η will be fixed for the duration of the paper. Note for later use that E, E_1, E_2 lie in the compact set $\{z : |z| \leq 1 - \eta\} \subset \mathbf{D}$.

To be as clear as possible about our assumptions on circle packings, we designate the following as Hypothesis (H).

Hypothesis (H) . *P is a circle packing by circles with mutually disjoint interiors having DL-complex K and such that: $E_2 \subset carr(P) \subset \Omega$; $mesh(P) < \eta$; and the euclidean radii ρ_i, ρ_j of any two circles of P satisfy the condition $\rho_i/\rho_j \leq \mathfrak{C}_r$.*

We continue to use the notations developed earlier related to the circle packing P — the path $\mathbf{r}(t)$, the graph G, conductances, transition probabilities, and so forth. Recall that there is a bound $\mathfrak{d}$ on $\deg(K)$ implied by the constant $\mathfrak{C}_r$. Our main concern will lie with nodes deep in the interior of K, so we establish the following notation:

Definition 8.2.1. *Let K^E (resp. K^{E_1}) denote the subcomplex of K formed by those faces lying in E (resp. E_1) when K is embedded as carr(P). Under Hypothesis (H), all nodes of K^E (resp. K^{E_1}) are interior nodes of K. Denote by G^E the subgraph of G formed by the standard nodes associated with K^E and their twins.*

Remark: The identification of K with carr(P) is convenient here for purposes of notation and later for obtaining combinatoric information about K. However, the reader is reminded that it is the packings $K(\mathbf{r}(t))$ which are ultimately of interest. Obviously they differ quantitatively from $K(\mathbf{r}(0)) = K(R)$, the hyperbolic complex for P, since the radii are different; but they also differ qualitatively, since $K(\mathbf{r}(t))$ may be associated with a configuration of circles involving global overlaps — in the terminology of [6], $K(\mathbf{r}(t))$ may fail to represent a "planar" circle packing. It is important to recognize this possibility, since it complicates some of our considerations. For example, the result of Lemma 8.3.2(i) below would follow easily from the Ring Lemma 2.3.1 if $K(\mathbf{r})$ were known to be planar. As it happens, however, the proof requires the technical Lemma 8.3.1.

8.3. **Bounds on Conductance.** We must establish uniform bounds on certain conductances and transition probabilities for the associated random walk on G. That first requires a replacement for $\mathfrak{C}_r$ in controlling the geometry of $K(\mathbf{r}(t))$: the circles of P are comparably sized by hypothesis, but we must prove that comparability persists as one moves towards the Andreev packing. Note that the results here involve hyperbolic radii and are needed only for vertices associated with a compact set.

Lemma 8.3.1. *There exist constants $\mathfrak{C}_1, \mathfrak{C}_2, \mathfrak{C}_3 \in (1, \infty)$, depending only on $\mathfrak{C}_r$, such that if P is a circle packing satisfying Hypothesis (H), and $\mathbf{r} = \mathbf{r}(t)$ is any radius vector on the path from R to $\widetilde{R}$, then*

(i). $1 \leq \widetilde{R}_j / r_j \leq \mathfrak{C}_1$ for every vertex $v_j \in K^{E_1}$,

(ii). $r_j / r_i \leq \mathfrak{C}_2$ for every pair of vertices $v_j, v_i \in K^{E_1}$, and

(iii). $r_j \leq \mathfrak{C}_3 \cdot mesh(P)$ for every vertex $v_j \in K^E$.

Proof: (i). By Propositions 7.2.2 and 5.3.1(c), $R_j \leq r_j \leq \widetilde{R}_j$, $\forall j$, so it suffices to treat the case $\mathbf{r} = R$; that is, one need only compare the sizes of circles of $\widetilde{P}$ to those of P. We work first with euclidean radii, and then convert to hyperbolic.

Fix attention on a vertex $v_j \in K^E$; let c_j denote the corresponding circle of P, ψ_j its euclidean center, and ρ_j its euclidean radius. Hypothesis (H) ensures that the euclidean disc $\{|z - \psi_j| < \eta\}$ lies in carr(P). Apply a Möbius transformation of $\mathbf{D}$ to $\widetilde{P}$ in order to place the circle for v_j at the origin; denote the circle by $\tilde{c}_j'$ and let $\tilde{\rho}_j$ denotes its euclidean radius. The Discrete Distortion Lemma of [14] gives

$$\tilde{\rho}_j / \rho_j \leq 1/\eta. \tag{10}$$

Now with regard to the hyperbolic radii: The hyperbolic radius $\widetilde{R}_j$ for $\tilde{c}'_j$ is bounded by $\sqrt{\mathfrak{d}}$ and since $\tilde{c}'_j$ is centered at the origin, $\widetilde{R}_j < \tilde{\rho}_j(2/(1-(1-\sqrt{\mathfrak{d}})^2)$. This, (10), and the fact that the hyperbolic radius of a circle exceeds its euclidean radius implies inequality (i) with $\mathfrak{C}_1 = \dfrac{2}{\eta(1-(1-\sqrt{\mathfrak{d}})^2)}$.

(ii). We are interested in comparing components of $\mathbf{r}$: Fix $v_i, v_j \in K^E$, and let ρ_i, ρ_j be the euclidean radii of their circles in P. Let $b = \dfrac{2}{1-(1-\eta)^2}$. In the following string of inequalities, we use successively: §5.3.1(c); the result (i) above; the comparability of euclidean and hyperbolic radii in $E_1 \subset \{|z| \leq 1-\eta\}$; Hypothesis (H); and finally the fact that the hyperbolic radius of a circle exceeds its euclidean radius.

$$r_i \;\leq\; \widetilde{R}_i \;\leq\; \mathfrak{C}_1 R_i \;\leq\; \mathfrak{C}_1 b\rho_i \;\leq\; \mathfrak{C}_1 b\,\mathfrak{C}_r\rho_j \;\leq\; \mathfrak{C}_1 b\,\mathfrak{C}_r r_j \ .$$

Setting $\mathfrak{C}_2 = \mathfrak{C}_1 b\,\mathfrak{C}_r$, we obtain the inequality of (ii).

(iii). Fix $v_j \in K^E$, and let b be the constant defined above. Then $R_j \leq b$ mesh (P). By result (i), $r_j \leq \widetilde{R}_j \leq \mathfrak{C}_1 R_j$. Setting $\mathfrak{C}_3 = \mathfrak{C}_1 b$, we obtain inequality (iii). □

We have been very loose with the constants here, but these will serve our purposes in the sequel. Note that we have disregarding the dependence of various constants on E and η since these are fixed throughout our proof of the Key Lemma. Next, we give the bounds on conductance.

Lemma 8.3.2. *There exist constants $\mathfrak{C}_4 > 1$ and $\mathfrak{C}_5 > 0$ depending only on $\mathfrak{C}_r$, so that if P be a circle packing satisfying Hypothesis (H), $\mathbf{r} = \mathbf{r}(t)$ is any radius vector on the path from R to $\widetilde{R}$, and v and w are neighboring vertices of K^E, then*

(i). $\mathfrak{C}_4^{-1} < \mathcal{C}_{vw} < \mathfrak{C}_4$,

(ii). $\mathcal{C}_{vv'} \to 0$ *as* mesh$(P) \to 0$, *and*

(iii). $p_{vw} \geq \mathfrak{C}_5$.

Proof: (i). Let v and w have common neighbors u, a, as in Figure 5. Lemma 8.3.1(ii) provides the constant $C = \mathfrak{C}_2$ giving the comparability of their s-radii, while §8.3.1(iii) gives a common bound B. By Definition 6.5.1,

$$\mathcal{C}_{vw} = h(w,u,a,v)\sqrt{v}(v-1) \ .$$

The conclusion of (i) is simply the statement of Lemma 4.4.1(iv).

For (ii), recall that

$$\mathcal{C}_{vv'} = \frac{\partial A_v}{\partial v}\sqrt{v}(v-1) \ . \tag{11}$$

Here A_v is the hyperbolic area of the star of v, and we write

$$\frac{\partial A_v}{\partial v} = \sum_j \frac{\partial a_j}{\partial v},$$

where the a_j denote the areas of the faces of this star. Consider without loss of generality that the area a_j is that of the face formed by v, w, u. By Lemma 4.4.3, $\dfrac{\partial a_j}{\partial v}$ is bounded by a constant C_4 which depends only on C and B. Since the sum involves at most $\mathfrak{d}$ faces, and since v goes to 1 as mesh(P) goes to zero, (ii) follows from (11).

For (iii), recall from (7) that $p_{vw} = \mathcal{C}_{vw}/\mathcal{C}_v$. The bounds from (i) and (ii) along with the bound $\mathfrak{d}$ on the number of edges from the vertex v provide the positive lower bound $\mathfrak{C}_5$ on p_{vw}. □

9. The Local Harnack Inequality

9.1. **Introduction.** Our aim is an inequality which will be applied in Section 10 to the weighted visitation function U. We start with routine probabilistic arguments proving that nonnegative discrete harmonic functions associated with a reversible Markov process will satisfy a version of the classical Harnack inequality. The more difficult task, however, is in showing that for the particular processes $\mathfrak{M}^b$ the constant of the inequality behaves properly as mesh size goes to zero, and it is here that one invokes the geometric hypotheses of the Main Theorem *via* the preliminaries of the previous section.

9.2. **The Statement.**

Lemma 9.2.1 (Local Harnack Inequality)**.** *There exists a constant $0 < \mathfrak{C}_h < \infty$, depending on mesh$(P)$ and $\mathfrak{C}_r$, so that the following holds: for every circle packing P satisfying Hypothesis (H), for every $\mathbf{r}(t), t \in [0,1)$, for every nonnegative function W on G which is harmonic for $\mathfrak{M}^b$, and for every pair v, w of neighboring vertices of G^E, the inequality $W(w)/W(v) \leq \mathfrak{C}_h$ holds. Moreover, $\mathfrak{C}_h \longrightarrow 1$ as mesh$(P) \longrightarrow 0$.*

The similarity to the classical Harnack inequality is not all that one would like. However, to put it in context, consider this statement in the unit disc:

Given a compact subset $E \subset \mathbf{D}$ and $\tau > 0$, there exists a constant $C > 1$ such that for any positive harmonic function h on $\mathbf{D}$ and any points $a, b \in E$ with $|a - b| < \tau$, the inequality $h(a)/h(b) \leq C$ holds; moreover, $C \longrightarrow 1$ as $\tau \longrightarrow 0$.

This, for instance, is sufficient for proving that there are no nonconstant positive harmonic functions on the euclidean plane. That is the image to keep in mind: the closer two points are, relative to the domain, the more uniformly comparable are the values of positive harmonic functions at those points.

9.3. **The Inequality.** The technique for proving existence of $\mathfrak{C}_h$ is motivated by [28, §13.P1]. Fix neighboring vertices v, w of K^E. We will consider these as nodes of G^E and study the random walk $\mathfrak{M}^b$ starting at v. (Note that $\mathfrak{M}^b$ is associated with $K(\mathbf{r}(t))$ for some $t \in [0,1)$.) Denote by S the set of absorbing nodes of G, namely, the twin nodes and the standard boundary nodes. Define the following collection of stopping times:

(a). τ_S is the hitting time for the absorbing set S.

(b). τ_w is the hitting time for the set $\{w\}$.

(c). $\tau = \tau_S \wedge \tau_w$ is the smaller of τ_S and τ_w.

(d). Define $\tau_0 \equiv 0$ and then inductively

$$\tau_{n+1} = \min\{k > \tau_n : \mathbf{X}_k \in S \cup \{v, w\}\},\ n = 0, 1, \cdots,$$

with $\tau_{n+1} = \infty$ if $\tau_n = \infty$.

Because almost every random walker will eventually be absorbed at a twin or boundary node, $\mathbf{P}_v[\tau_S < \infty] = 1$, and hence $\mathbf{P}_v[\tau < \infty] = 1$. By Lemma 6.7.4, we have

$$W(v) = \mathbf{E}_v[W(\mathbf{X}_\tau)] = W(w) \cdot \mathbf{P}_v[\tau = \tau_w] + W(\mathbf{X}_{\tau_S}) \cdot \mathbf{P}_v[\tau = \tau_S]. \tag{12}$$

Our interest is in a lower bound on $\mathbf{P}_v[\tau = \tau_w]$; we obtain it by looking at random walkers between return visits to v.

Because the τ_n are stopping times, the following probabilities are well defined, independent of n:

$$\begin{aligned} a &= \mathbf{P}_v[\mathbf{X}_{\tau_{n+1}} = w \mid \mathbf{X}_{\tau_n} = v], \\ b &= \mathbf{P}_v[\mathbf{X}_{\tau_{n+1}} = v \mid \mathbf{X}_{\tau_n} = v], \\ c &= \mathbf{P}_v[\mathbf{X}_{\tau_{n+1}} \in S \mid \mathbf{X}_{\tau_n} = v]. \end{aligned}$$

They represent the probabilities that, upon leaving v, a random walker first hits the set $S \cup \{v, w\}$ at w, v, or S, respectively. These events are mutually exclusive, and omit only the possibility that $[\tau_{n+1} = \infty]$, which has probability zero; therefore, $a+b+c = 1$.

Using standard properties of conditional probabilities, we have

$$\begin{aligned} \mathbf{P}_v[\mathbf{X}_\tau = w] &\geq \mathbf{P}_v[\mathbf{X}_{\tau_1} = w] \\ &\quad + \sum_n \big(\mathbf{P}_v[\mathbf{X}_{\tau_{n+1}} = w \mid \mathbf{X}_{\tau_n} = v] \cdot \prod_{j=1}^{n} \mathbf{P}_v[\mathbf{X}_{\tau_j} = v \mid \mathbf{X}_{\tau_{j-1}} = v]\big) \\ &= a + a \cdot b + a \cdot b^2 + \cdots = a\,(\frac{1}{1-b}) \\ &= \frac{a}{a+c}\ . \end{aligned}$$

The probability that a random walker hits w immediately upon leaving v is the transition probability p_{vw}, so $a \geq p_{vw}$. Under Hypothesis (H) and applying Lemma 8.3.1(ii) and Lemma 8.3.2(iii), this transition probability exceeds $\mathfrak{C}_5$. Also, it is clear from the definitions that $c < p^v_{\text{esc}}$, where p^v_{esc} denotes the escape probability to S from v. Putting these facts together gives

$$\mathbf{P}_v[\mathbf{X}_\tau = w] > \frac{a}{a + p^v_{\text{esc}}} > \frac{\mathfrak{C}_5}{\mathfrak{C}_5 + p^v_{\text{esc}}}.$$

Returning to (12) and noting that $W(\mathbf{X}_{\tau_S}) \geq 0$, we obtain the inequality

$$W(v) > W(w) \cdot \frac{\mathfrak{C}_5}{\mathfrak{C}_5 + p^v_{\text{esc}}} \ .$$

The Harnack inequality will therefore hold with constant

$$\mathfrak{C}_h = \sup_{v \in K^E} \frac{\mathfrak{C}_5 + p^v_{\text{esc}}}{\mathfrak{C}_5} > 1 \ . \tag{13}$$

9.4. **Dependence on Mesh Size.** It remains to show that $\mathfrak{C}_h$ goes to 1 as mesh (P) goes to zero. By (13), it suffices to prove that the escape probabilities p^v_{esc} go to zero uniformly for $v \in K^E$. Though it would be preferable to prove this directly with estimates, the only argument we have uses diagonalization to arrive at a contradiction; so we work with sequence of circle packings.

Assumption 9.4.1. *Assume that there exists $\beta > 0$ and a sequence $\{P_n\}$ of circle packings satisfying Hypothesis (H) so that mesh (P_n) goes to zero but*

$$p^{(n)}_{esc} > \beta. \tag{14}$$

That is, for each n there is the Markov process $\mathfrak{M}^b_n$ associated with some stage of the evolution of P_n towards its Andreev packing; a designated node $v^{(n)} \in G^E_n$; and the concomitant escape probability $p^{(n)}_{esc}$ from $v^{(n)}$ to the absorbing nodes of G_n so that (14) holds.

Note that for each n, the process $\mathfrak{M}^b_n$ is associated with $K_n(\mathbf{r}(t_n))$ for some $t_n \in [0, 1)$. There is no relationship assumed between the parameters t_n for different values of n. Likewise, there is no relationship assumed between the nodes $v^{(n)}$ — we simply require that $v^{(n)}$ belong to G^E_n.

We work towards a contradiction in stages: Based on Assumption 9.4.1, we first extract a finite graph and an associated limiting random walk from the sequence of processes $\mathfrak{M}^b_n$. Next, we compare this to the simple random walk on the same graph. This we compare in turn to the simple random walk on a regular 2-dimensional lattice. The properties of this last process are very well known, and it is here that we reach a contradiction with a famous result of Pólya.

9.5. **Stage I.** Fix an integer $m > 2$. We start by constructing a finite graph N_m which embeds in infinitely many of the graphs $\{G_n\}$.

It is best to work geometrically; in the following discussion, we will identify K_n with its geometric realization as carr (P_n). A vertex $w \in K_n$ is said to be in **generation** k if k is the smallest number of edges in an edge path from w to the distinguished vertex $v^{(n)}$. Let L denote the subcomplex of K_n spanned by the vertices of generation no greater than m; that is, L contains these vertices, all edges bounded by pairs of these vertices, and all faces bounded by triples of these edges. Incorporate any "islands",

subcomplexes of the complement of L which L separates from the boundary vertices of K_n. The resulting simply connected subcomplex of K_n is denoted K_n^m.

By Hypothesis (H), $E_2 \subset K_n$, while the designated vertex $v^{(n)}$ is in E. We may assume henceforth that n is sufficiently large that $\text{mesh}\,(P_n) < \eta/2m$. This implies first that all boundary vertices of K_n must be of generation greater than m and second that the vertices of K_n of generation up to and including m lie in E_1. Since E_1 is a Jordan region, $K_n^m \subset E_1$. Note for later reference that the vertices of ∂K_n^m are precisely generation m.

We claim that the number of vertices of K_n^m is bounded, the bound depending only on m and $\mathfrak{C}_r$: The uniform bound $\mathfrak{d}$ on the degree of vertices of K_n easily implies uniform bounds on the number of vertices of L and on the number of edges in the boundary of L. The latter, in turn, implies a uniform bound on the number of islands which must be adjoined to L in forming K_n^m. The vertices in these islands are of generation greater than m. There is no combinatoric reason for a bound on their number, but there is a geometric one related to $\mathfrak{C}_r$. Namely, the circles of P_n associated with the vertices of an island must be comparable in size to the circles associated with the surrounding boundary of L. We already noted a uniform bound on the number of the latter, implying a uniform bound on the number of the former. All together then, we have a bound on the number of vertices of K_n^m.

Standard arguments imply that *the subcomplex K_n^m is simplicially equivalent to one of only finitely many complexes, independent of n.* In conjunction with this, the Pigeon Hole Principle implies that there exists an infinite collection of indices $\{n_j\}$ so that the subcomplexes $K_{n_j}^m$ are simplicially equivalent to one another. The 1-skeleton of this common (abstract) subcomplex will be denoted N_m and will be the graph of interest. By throwing out the other indices, we may assume henceforth that N_m embeds in the 1-skeleton of K_n for every n and spans a simply connected subcomplex of K_n. It has an "origin" ν which corresponds for each n with the designated vertex $v^{(n)} \in K_n^E$ and a "boundary" ∂N_m which correspond for each n with ∂K_n^m.

Though N_m is an abstract graph, it embeds geometrically in $\text{carr}\,(P_n)$, it embeds simplicially in K_n, and it embeds as a subgraph of standard nodes from G_n. We move freely among these various identifications as we proceed. The essential properties of N_m are these:

(a). ν belongs to at least three edges of N_m.

(b). ∂N_m consists of nodes of generation m from ν.

(c). ∂N_m separates $v^{(n)}$ from ∂G_n.

(d). The nodes of N_m embed in K_n as vertices of $K_n^{E_1}$.

As a subgraph of G_n, N_m contains the first m generations of standard nodes about $v^{(n)}$. We use conductances to define the random walk on N_m as a limit of the restrictions

to N_m of the random walks $\mathfrak{M}_n^b$. Focus on neighboring nodes v, w of N_m. By property (d) above, Lemma 8.3.1(i) and Lemma 8.3.2(i), the corresponding edge in G_n has a conductance $\mathcal{C}_{vw}^{(n)}$ satisfying $\mathfrak{C}_4^{-1} \leq \mathcal{C}_{vw}^{(n)} \leq \mathfrak{C}_4$. Since there are finitely many edges in N_m, we can assume (*via* diagonalization and extraction of a subsequence) that

$$\widehat{\mathcal{C}}_{vw} = \lim_{n\to\infty} \{\mathcal{C}_{vw}^{(n)}\}$$

exists for every edge (v, w) of N_m. It is immediate that the numbers $\widehat{\mathcal{C}}_{vw}$ satisfy companion properties to the original conductances; namely

$$\mathfrak{C}_4^{-1} \leq \widehat{\mathcal{C}}_{vw} \leq \mathfrak{C}_4, \qquad \widehat{\mathcal{C}}_{vw} = \widehat{\mathcal{C}}_{wv}, \quad v, w \in N_m.$$

Put $\widehat{\mathcal{C}}_{vw} = 0$ if v and w are not neighbors. As we have done before, we use these to prescribe a random walk on N_m: Define the node conductances $\widehat{\mathcal{C}}_v = \sum_{w\in N} \widehat{\mathcal{C}}_{vw}, v \in N_m$. Then

$$q_{vw} = \widehat{\mathcal{C}}_{vw}/\widehat{\mathcal{C}}_v, \ v, \ w \in N_m$$

defines the collection of transition probabilities for a reversible Markov process on N_m.

Our interest is in the escape probability from ν to ∂N_m, to be denoted p_{esc}^I. Recall that the conductance for $\mathfrak{M}_n^b$ at a node $v \in G_n$ is given by

$$\mathcal{C}_v^{(n)} = \mathcal{C}_{vv'}^{(n)} + \sum_w \mathcal{C}_{vw}^{(n)}.$$

By Lemma 8.3.2(ii), the conductance $\mathcal{C}_{vv'}^{(n)}$ to the absorbing twin goes to zero as mesh goes to zero; putting all of this together gives

$$q_{vw} = \frac{\widehat{\mathcal{C}}_{vw}}{\widehat{\mathcal{C}}_v} = \lim_n \frac{\mathcal{C}_{vw}^{(n)}}{\mathcal{C}_v^{(n)}} = \lim_n p_{vw}^{(n)}, \ v, \ w \in N_m. \tag{15}$$

We can use this to get a bound on p_{esc}^I. The escape probability $p_{\text{esc}}^{(n)}$ for $\mathfrak{M}_n^b$ is the probability that a random walker starting at $v^{(n)}$ will be absorbed at a twin or boundary node of G_n before returning to $v^{(n)}$. By (c) above, if we modify this escape probability by replacing the condition "hit the boundary of G_n" by "hit a node of ∂N_m", it can only increase. It is immediate from (15) and the lower bound β on the escape probabilities for the G_n, that $p_{\text{esc}}^I > \beta > 0$. This completes Stage I, and we summarize.

Summary I . *Under Assumption 9.4.1 and given $m > 2$, there exists a graph N_m with the following properties:*

(a). N_m has a designated node ν and a designated boundary ∂N_m whose nodes are combinatoric distance m from ν.

(b). There exist circle packings P satisfying Hypothesis (H) and having arbitrarily small mesh so that N_m may be embedded in the 1-skeleton of the associated complex K. In this embedding, ν is mapped to a vertex of K^E and the embedded image of N_m contains all vertices of K whose combinatoric distance from ν is no greater than m.

(c). There is a reversible random walk defined on N_m whose associated edge conductances lie in $[\mathfrak{C}_4^{-1}, \mathfrak{C}_4]$ and whose escape probability from ν to ∂N_m satisfies $p^I_{esc} > \beta$.

9.6. **Stage II.** Our next objective is to move from the limiting random walk defined on N_m above to the simple random walk on N_m. The comparison reflects **the irrelevance of bounded twiddling** (see [11, §8.3]) and relies on Rayleigh's Monotonicity Law.

For our particular application, let $\mathbf{C}$ be the collection of limiting conductances on the edges of N_m derived in the previous subsection and let $\mathbf{C}'$ be the collection of constant conductances, having value $\mathfrak{C}_4$ for each edge. The former gives the random walk of Summary I, while the latter gives the simple random walk. Let $p^I_{\rm esc}$ and $p^{II}_{\rm esc}$, respectively, denote the escape probabilities from ν to ∂N_m. By Summary I, $\mathbf{C} \le \mathbf{C}'$, so the monotonicity law implies $\mathcal{C}_{\rm EFF} \le \mathcal{C}'_{\rm EFF}$.

The node ν has degree at least 3 and at most $\mathfrak{d}$. In particular, the node conductances at ν satisfy

$$\mathcal{C}_\nu \ge 3\mathfrak{C}_4^{-1}, \qquad \mathfrak{C}_4\mathfrak{d} \ge \mathcal{C}'_\nu.$$

Computing escape probabilities, we have

$$p^I_{\rm esc} = \frac{\mathcal{C}_{\rm EFF}}{\mathcal{C}_\nu} \le \frac{\mathfrak{C}_4\mathcal{C}_{\rm EFF}}{3} \le (\frac{\mathfrak{C}_4^2\mathfrak{d}}{3})(\frac{\mathcal{C}'_{\rm EFF}}{\mathcal{C}'_\nu}) = (\frac{\mathfrak{C}_4^2\mathfrak{d}}{3})p^{II}_{\rm esc}.$$

With the information on $p^I_{\rm esc}$ from Summary I, this completes Stage II and we may summarize.

Summary II . *Under Assumption 9.4.1 and given $m > 2$, there exists a graph N_m so that conditions (a) and (b) from Summary I hold and so that the escape probability from ν to ∂N_m for the simple random walk satisfies*

$$p^{II}_{esc} > (\frac{\mathfrak{C}_4^2\mathfrak{d}}{3})\beta.$$

9.7. **Stage III.** Our final objective is to move from the simple random walk on N_m to the simple random walk on a more regular and well understood graph.

Definition 9.7.1. *Let $\mathbf{Z}^2$ denote the infinite graph formed by the 2-dimensional lattice of points in the plane having integer coordinates, with horizontal and vertical neighbors connected by edges. Denote by $\mathbf{0}$ the node of $\mathbf{Z}^2$ at the origin.*

*For a positive integer k, the k-**fuzz** of $\mathbf{Z}^2$, denoted $\mathbf{Z}^2_k$, is the graph obtained from $\mathbf{Z}^2$ by introducing an edge between any two nodes which are a combinatoric distance no more than k apart in $\mathbf{Z}^2$ and are not already connected by an edge.*

The constant $\mathfrak{C}_r$ enters again in a crucial way in showing that the graph N_m of Stages I and II can be embedded in $\mathbf{Z}^2_k$ for a positive integer k which is independent of m. Behind this is another notion taken from [11], namely that of a **civilized embedding**.

Lemma 9.7.2. *Let $\mathfrak{k}$ denote the smallest integer which exceeds $8\sqrt{2}\,\mathfrak{C}_r$. Then for any integer $m > 2$, N_m can be embedded in $\mathbf{Z}^2_{\mathfrak{k}}$, with ν mapped to $\mathbf{0}$. Moreover, given any*

positive integer n, if $m \geq 4n^2\mathfrak{k}^2$, then the nodes of ∂N_m are combinatoric distance at least n from $\mathbf{0}$ in $\mathbf{Z}^2_{\mathfrak{k}}$.

Proof: By Summary I, N_m may be identified with a subgraph in the complex K of some circle packing P satisfying Hypothesis (H). P itself is not important here, but N_m gets carried along when we embed K as $\mathrm{carr}\,(P)$, and we get additional information about N_m from this geometric setting.

We compare the geometric version of N_m with a scaled version of $\mathbf{Z}^2$. Contract $\mathbf{Z}^2$ by the euclidean scaling factor $s = \dfrac{\mathrm{mesh}\,(P)}{2\mathfrak{C}_r}$ and denote the resulting graph by $\mathfrak{Z}^2$. Neighboring nodes of $\mathfrak{Z}^2$ are (euclidean) distance s apart, and no circle of P has radius less than $s/2$; so this scaling ensures that every circle of P contains a node of $\mathfrak{Z}^2$. Identify each node of N_m with a node of $\mathfrak{Z}^2$ lying in the corresponding circle of P. Nodes of $\mathfrak{Z}^2$ lying in tangent circles of P are within euclidean distance $4 \cdot \mathrm{mesh}\,(P)$ of one another, so their combinatoric distance in $\mathfrak{Z}^2$ can be no more than $8\sqrt{2}\,\mathfrak{C}_r \leq \mathfrak{k}$. Thus, nodes of N_m sharing an edge will be identified with nodes of $\mathfrak{Z}^2$ which share an edge in the $\mathfrak{k}$-fuzz of $\mathfrak{Z}^2$. Clearly, the $\mathfrak{k}$-fuzz of $\mathfrak{Z}^2$ can be identified with $\mathbf{Z}^2_{\mathfrak{k}}$ so that ν is identified with $\mathbf{0}$. This proves the first part of the lemma.

Now assume $n > 0$ and fix $m > 16n^2\mathfrak{k}^2$. By Summary I(b), we may assume without loss of generality that $\mathrm{mesh}\,(P)$ is so small that $n\mathfrak{k}s < \eta/2$. Let Δ_1 and Δ_2 denote the discs of radius $n\mathfrak{k}s$ and $2n\mathfrak{k}s$, respectively, centered at ν. Any nodes of N_m which are combinatoric distance n or less from $\mathbf{0}$ in $\mathbf{Z}^2_{\mathfrak{k}}$, are associated with circles of P which intersect Δ_1. We argue that these must be of combinatoric distance less than m from ν in N_m; in particular, none can be belong to ∂N_m.

The circles of P are comparably sized, with none having euclidean radius less than $s/2$, but this alone is not enough to ensure that later generation circles of P cannot be geometrically close to ν. We also need the fact that the circles associated with N_m fill up a region around ν: Recall that ν was chosen to be a vertex of K^E; in particular, $\Delta_2 \subset \mathrm{carr}\,(P)$. The circles of P are non-overlapping and have radii at least $s/2$, so by euclidean area considerations, P has no more than $16n^2\mathfrak{k}^2$ of its circles lying in Δ_2. It is therefore evident that any circle touching Δ_1 can be reached from ν by chain of less than $16n^2\mathfrak{k}^2$ circles. □

Definition 9.7.3. *Given a positive integer n, define Z_n to be the subgraph of $\mathbf{Z}^2_{\mathfrak{k}}$ consisting of the first n generations about node $\mathbf{0}$, with ∂Z_n denoting the nodes of precisely generation n.*

Fixing $n > 0$ and $m = 16n^2\mathfrak{k}^2$, we are now in position to compare escape probabilities: Define $M_n = N_m \cap Z_n$ and $\partial M_n = N_m \cap \partial Z_n$. All the random walks we consider are simple random walks and the escape probabilities are escapes from $\mathbf{0}$ to the designated boundary. Let q_{esc} denote the escape probability for M_n and $p^{III}_{\mathrm{esc}} = p^{III}_{\mathrm{esc}}(n)$ the escape probability for Z_n. We do the comparisons in two steps:

First, consider M_n as a subgraph of N_m. By our choice of m and the last part of Lemma 9.7.2, a random walker on M_n starting at $\mathbf{0}$ will necessarily hit ∂M_n before

hitting ∂N_m. By Summary II this implies

$$q_{\rm esc} > p_{\rm esc}^{II} > (\frac{\mathfrak{C}_4^2 \mathfrak{d}}{3})\beta \ . \tag{16}$$

Next, consider M_n as embedded in Z_n. Since $\partial M_n \subset \partial Z_n$, we can compare effective conductances. Our random walks are simple, so the transition probabilities are associated with unit conductances for all edges of Z_m. Write $\mathcal{C}_{\rm EFF}^M$ and $\mathcal{C}_{\rm EFF}^Z$ for the effective conductances from $\mathbf{0}$ to ∂M_n and to ∂Z_n, respectively. By Rayleigh's Monotonicity Law, we can only increase the effective conductance by adding to M_n those edges of Z_n which it lacks, so $\mathcal{C}_{\rm EFF}^M \leq \mathcal{C}_{\rm EFF}^Z$. There are at least three edges from $\mathbf{0}$ in M_n and precisely $2\mathfrak{k}(\mathfrak{k}+1)$ edges from $\mathbf{0}$ in $Z_n \subset \mathbf{Z}_{\mathfrak{k}}^2$. Therefore

$$p_{\rm esc}^{III} = \frac{\mathcal{C}_{\rm EFF}^Z}{2\mathfrak{k}(\mathfrak{k}+1)} \geq \frac{\mathcal{C}_{\rm EFF}^M}{2\mathfrak{k}(\mathfrak{k}+1)} = (\frac{\mathcal{C}_{\rm EFF}^M}{3})(\frac{3}{2\mathfrak{k}(\mathfrak{k}+1)}) \geq (\frac{3}{2\mathfrak{k}(\mathfrak{k}+1)})q_{\rm esc} \ . \tag{17}$$

Combining the inequalities (16) and (17), we may now summarize

Summary III . *Under Assumption 9.4.1, given $n > 0$, the escape probability from $\mathbf{0}$ to ∂Z_n for the simple random walk on Z_n, denoted $p_{esc}^{III}(n)$, satisfies*

$$p_{esc}^{III}(n) > (\frac{3}{2\mathfrak{k}(\mathfrak{k}+1)})\,(\frac{\mathfrak{C}_4^2 \mathfrak{d}}{3})\beta \ .$$

9.8. **The Contradiction.** We can now see a contradiction with a celebrated result of Pólya regarding the behavior of simple random walks on the regular rectangular d-dimensional lattices $\mathbf{Z}^d$, $d = 1, 2, 3, \cdots$. A simple random walk on an infinite graph is **recurrent** if random walkers will return to their starting nodes with probability one, otherwise it is said to be **transient**.

Theorem 9.8.1 (Pólya's Theorem [25])**.** *The simple random walk is recurrent on $\mathbf{Z}^1$ and $\mathbf{Z}^2$ and transient on $\mathbf{Z}^d$ for $d \geq 3$.*

Our interest is in the 2-dimensional case only, and we require three additional results, for which we refer the reader again to Doyle and Snell [11, Chps. 5, 8]:

(1). It can be shown that the $\mathfrak{k}$-fuzz of $\mathbf{Z}^2$, what we have denoted $\mathbf{Z}_{\mathfrak{k}}^2$, is also recurrent.

(2). This can be reformulated in terms of escape probabilities: The escape probability for $\mathbf{Z}_{\mathfrak{k}}^2$, call it $\mathfrak{p}_{\rm esc}$, is the probability that a random walker starting at $\mathbf{0}$ will never return to $\mathbf{0}$. Recurrence is equivalent to $\mathfrak{p}_{\rm esc} = 0$.

(3). The escape probability $\mathfrak{p}_{\rm esc}$ is the limit as n goes to infinity of the escape probabilities to the $n^{\rm th}$ generation of $\mathbf{Z}_{\mathfrak{k}}^2$. These are precisely the escape probabilities from the graphs Z_n discussed in the previous section and denoted $p_{\rm esc}^{III}(n)$.

However, under Assumption 9.4.1, Summary III tells us that

$$\mathfrak{p}_{\text{esc}} = \lim_n p_{\text{esc}}^{III}(n) > \frac{3}{2\mathfrak{k}(\mathfrak{k}+1)}(\frac{\mathfrak{C}_4^2\mathfrak{d}}{3})\beta > 0.$$

This is contrary to (1) and (2), and hence contradicts Pólya's Theorem. We conclude that the Assumption 9.4.1 is untenable, and our proof of the Local Harnack Inequality is complete. □

Remark: The work of this section has been necessitated by the lack of an infinite supercomplex containing all the complexes K_n, as is provided by K_H in the hexagonal case (see §1.4). The simple random walk on K_H is recurrent, and consequently its positive harmonic functions are constant. The sense of this section is that on our irregular graphs the random walks are "recurrent in the limit."

10. Proof of the Key Lemma

10.1. **Introduction.** We prove the Key Lemma *via* the Reduction 3.2.1. Given a circle packing P satisfying Hypothesis (H), consider a mutually tangent triple (c_0, c_1, c_2) of circles lying in E and the corresponding triple $(\tilde{c}_0, \tilde{c}_1, \tilde{c}_2)$ of $\widetilde{P}$. Let T and $\widetilde{T}$ denote the faces they form in $\text{carr}\,(P)$ and $\text{carr}\,(\widetilde{P})$, respectively. We need to show that each angle of T is close to the corresponding angle of $\widetilde{T}$ when P has sufficiently small mesh. One complication remains before we apply our machinery — we need to measure angles in the hyperbolic setting.

10.2. **Hyperbolic Angles.** In addition to the euclidean triangles T and $\widetilde{T}$, the triple (c_0, c_1, c_2) and its counterpart in $\widetilde{P}$ form hyperbolic triangles T^h and $\widetilde{T}^h$, respectively. First, let us compare T to T^h: Because c_0, c_1, c_2 lie in the compact set E, $\text{mesh}\,(P)$ small implies that these circles have small hyperbolic radii and that T^h has small hyperbolic diameter. Applying Lemma 4.2.4, we can make the angles of T as close to those of T^h as we wish by making $\text{mesh}\,(P)$ small. A similar strategy in $\widetilde{P}$ requires the following geometric result.

Lemma 10.2.1. *There exists τ, $0 < \tau \leq \eta$, so that the following holds: If P satisfies Hypothesis (H), $\widetilde{P}$ is its Andreev packing, and $f_P : carr(P) \longrightarrow carr(\widetilde{P})$ is the normalized simplicial homeomorphism (see §2.2), then $f_P(E) \subset \{w : |w| \leq 1 - \tau\}$.*

Proof: We proved in Section 2.3 that f_P is κ-quasiconformal on $\text{int}(\text{carr}\,(P))$, where κ depends only on the constant $\mathfrak{C}_r$ of Hypothesis (H). Denote by Σ the open component of $\text{carr}\,(P)\backslash E$ which forms a (topological) annulus separating E from Ω^c. Since Σ contains the fixed annulus $E_2\backslash E$, its conformal module $\text{Mod}\,(\Sigma)$ is bounded below by some $C > 0$, independent of P. It is well known (see [23, §I.7]) that

$$\text{Mod}\,(f_P(\Sigma)) > C/\kappa. \tag{18}$$

Let $\rho = \sup\{|w| : w \in f_P(E)\}$ and let $w_0 \in E$ so that $|f(w_0)| = \rho$. By our assumptions and normalizations, $0 \in E$ and $f_P(0) = 0$. Therefore, $f_P(\Sigma)$ lies in $\mathbf{D}$ and separates 0 and w_0 from $\partial\mathbf{D}$, and we may compare it to the standard Grötzsch extremal domain $B(\rho) = \mathbf{D}\backslash\{z : 0 \le z \le \rho\}$ (see [23, §II.1]). In particular,

$$\text{Mod}\,(f_P(\Sigma)) \le \text{Mod}\,(B(\rho)) = \mu(\rho), \tag{19}$$

where μ is Grötzsch's module function. It is known that $\mu : [0,1] \to [0,\infty]$ is one-to-one, onto, and strictly decreasing. Comparing (18) and (19), we may choose

$$\tau = \min\{\eta, \mu^{-1}(C/\kappa)\},$$

and the proof is complete. □

We are now in position to compare $\widetilde{T}$ and $\widetilde{T}^h$: By Lemma 8.3.1(iii), when mesh (P) is small and because the circles c_0, c_1, c_2 are associated with vertices of K^E, the hyperbolic radii of $\tilde{c}_0, \tilde{c}_1, \tilde{c}_2$ are small. By the previous lemma, the circles forming $\widetilde{T}$ and $\widetilde{T}^h$ lie in the compact set $\{w : |w| \le 1 - \tau\}$, independent of P. Another application of Lemma 4.2.4 therefore implies that we can make the angles of $\widetilde{T}$ as close to those of $\widetilde{T}^h$ as we wish by making mesh (P) small.

10.3. **Reduction and Proof.** In view of the above, we can dispense with comparing T to $\widetilde{T}$ and work entirely with the hyperbolic triangles T^h and $\widetilde{T}^h$. To establish notation, suppose v, u, w are vertices of K^E forming a face and $\psi(t)$ is the resulting angle at v in the hyperbolic complex $K(\mathbf{r}(t))$, $0 \le t \le 1$. Thus, $\psi(0)$ is the angle in T^h while $\psi(1)$ is the angle in $\widetilde{T}^h$. The proof of the Key Lemma has now been reduced to the proof of the following.

Lemma 10.3.1. *Given $\epsilon > 0$, there exists $\delta > 0$ so that the following holds: If P satisfies Hypothesis (H) and if $\psi(t)$ is an angle associated with K^E as described above, then mesh $(P) < \delta$ implies $|\psi(1) - \psi(0)| < \epsilon$.*

Proof: Fix P satisfying Hypothesis (H). Recall that $\mathbf{r}(t)$ is a continuous path of radius vectors from the radii $R = \mathbf{r}(0)$ associated with P to the radii $\widetilde{R} = \mathbf{r}(1)$ associated with $\widetilde{P}$. The angle ψ depends on the radii for v, u, w via the Cosine Rule, so ψ is continuous. Moreover, the entries of $\mathbf{r}(t)$ are finite and differentiable for $0 \le t < 1$, so $\psi(t)$ is differentiable on $[0, 1)$. We establish the conclusion by showing that

$$|\psi(1) - \psi(0)| \le \int_0^1 |\frac{d\psi}{dt}(t)|dt < \epsilon.$$

Our situation is illustrated in Figure 7. We will adhere largely to the notations established earlier. However, as ψ depends on the radii at only three vertices, we find it convenient to use names rather than rely on the earlier indices. The hyperbolic area of the face containing ψ is A; the angle sums at v, u, w are $\theta_v, \theta_u, \theta_w$, respectively. As in earlier computations, we use v, u, w to designate both the vertices and their s-radii;

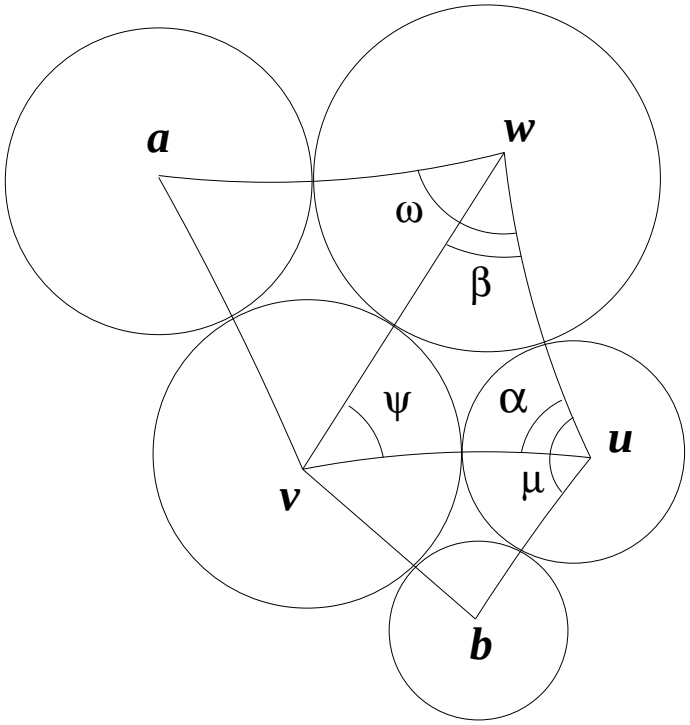

FIGURE 7. Setting for computations.

we use r_v, r_w, r_u to denote their hyperbolic radii. Finally, note that all these quantities are functions of t.

The auxiliary function $g(x, y, z)$ of §4.3.2 gives the angle at the vertex for x in a hyperbolic triangle formed by circles with s-radii x, y, z; its partials are g_1, g_2, and g_3. In the setting of Figure 7, we have

$$\psi = g(v, u, w), \qquad \alpha = g(u, v, w), \qquad \beta = g(w, u, v),$$

$$A = \pi - g(v, u, w) - g(u, v, w) - g(w, u, v).$$

Our estimate of $\dfrac{d\psi}{dt}$ is obtained with the aid of a comparison to $\dfrac{dA}{dv}\dfrac{dv}{dt}$. The bound δ will be determined in stages during the development, and will be assumed *a postiori* as a condition on the mesh size of P.

First, the computations involving ψ: Of course, the s-radii v, u, and w depend on t and have differentials computed earlier as part of $d\mathbf{r}$. Since $\psi = g(v, u, w)$, we have

$$\frac{d\psi}{dt} = g_1(v, u, w)\frac{dv}{dt} + g_2(v, u, w)\frac{du}{dt} + g_3(v, u, w)\frac{dw}{dt} \ .$$

We recall the visitation distribution V and its relationship to $\mathbf{r}$ from Proposition 7.2.2:

$$V_u = \big(\frac{\partial\theta_u}{\partial r_u}\big)\frac{dr_u}{dt} = \big(\frac{\partial\theta_u}{\partial u}\big)\frac{du}{dt}, \qquad V_w = \big(\frac{\partial\theta_w}{\partial r_w}\big)\frac{dr_w}{dt} = \big(\frac{\partial\theta_w}{\partial w}\big)\frac{dw}{dt} \ .$$

Substitution gives the final form

$$\frac{d\psi}{dt} = g_1(v,u,w)\frac{dv}{dt} + g_2(v,u,w)\big(\frac{\partial\theta_v}{\partial v}\big)^{-1}V_u + g_3(v,u,w)\big(\frac{\partial\theta_w}{\partial w}\big)^{-1}V_w \ .$$

Next, the computations involving A: Here we proceed differently; as the notation is intended to suggest, we treat A as a function of the radius at v only, keeping u and w constant.

$$\frac{dA}{dv}\frac{dv}{dt} = -g_1(v,u,w)\frac{dv}{dt} - g_2(u,v,w)\frac{dv}{dt} - g_3(w,u,v)\frac{dv}{dt} \ . \tag{20}$$

In an important series of computations, we now convert this to a more useful form. First, using the notation established in Figure 7 and the geometric significance of the auxiliary function h (see §4.3), note that

$$\frac{\partial\theta_w}{\partial v} = \frac{\partial\omega}{\partial v} = h(w,a,u,v) \ , \qquad \frac{\partial\theta_u}{\partial v} = \frac{\partial\mu}{\partial v} = h(u,w,b,v) \ ,$$
$$\frac{\partial\theta_v}{\partial w} = h(v,a,u,w) \ , \qquad \frac{\partial\theta_v}{\partial u} = h(v,b,w,u) \ .$$

Now apply identity (1) with appropriate identifications of s-radii from Figure 7 to get

$$g_2(u,v,w) = g_2(v,u,w)h(u,b,w,v)[h(v,b,w,u)]^{-1},$$
$$g_3(w,u,v) = g_3(v,u,w)h(w,a,u,v)[h(v,a,u,w)]^{-1}.$$

Finally, recall the definitions of the transition probabilities from §6.4.1 to verify

$$\big(\frac{\partial\theta_u}{\partial v}\big)\big(\frac{\partial\theta_v}{\partial u}\big)^{-1} = \big(\frac{\partial\theta_u}{\partial u}\big)^{-1}\big(\frac{\partial\theta_v}{\partial v}\big)\big(\frac{p_{vu}}{p_{uv}}\big) \ ,$$
$$\big(\frac{\partial\theta_w}{\partial v}\big)\big(\frac{\partial\theta_v}{\partial w}\big)^{-1} = \big(\frac{\partial\theta_w}{\partial w}\big)^{-1}\big(\frac{\partial\theta_v}{\partial v}\big)\big(\frac{p_{vw}}{p_{wv}}\big) \ .$$

Putting these together gives

$$\begin{aligned}\frac{dA}{dv}\frac{dv}{dt} = &- g_1(v,u,w)\frac{dv}{dt} \\ &- g_2(v,u,w)\big(\frac{\partial\theta_u}{\partial u}\big)^{-1}\big(\frac{\partial\theta_v}{\partial v}\big)\big(\frac{p_{vu}}{p_{uv}}\big)\frac{dv}{dt} \\ &- g_3(v,u,w)\big(\frac{\partial\theta_w}{\partial w}\big)^{-1}\big(\frac{\partial\theta_v}{\partial v}\big)\big(\frac{p_{vw}}{p_{wv}}\big)\frac{dv}{dt} \ .\end{aligned} \tag{21}$$

An important feature to note in comparing expressions (20) and (21) is the order of the arguments occurring in the various partials of g. Substituting once more using the

visitation distribution V, we get

$$\begin{aligned}\frac{dA}{dv}\frac{dv}{dt} = &- g_1(v,u,w)\frac{dv}{dt} \\ &- g_2(v,u,w)\big(\frac{\partial\theta_u}{\partial u}\big)^{-1}\big(\frac{V_v p_{vu}}{V_u p_{uv}}\big)V_u \\ &- g_3(v,u,w)\big(\frac{\partial\theta_w}{\partial w}\big)^{-1}\big(\frac{V_v p_{vw}}{V_w p_{wv}}\big)V_w \ .\end{aligned}$$

Addition and regrouping gives

$$\begin{aligned}|\frac{d\psi}{dt} + \frac{dA}{dv}\frac{dv}{dt}| \le &|g_2(v,u,w)\big(\frac{\partial\theta_u}{\partial u}\big)^{-1}\big[\,1 - \big(\frac{V_v p_{vu}}{V_u p_{uv}}\big)\,\big]V_u| \\ &+ |g_3(v,u,w)\big(\frac{\partial\theta_w}{\partial w}\big)^{-1}\big[\,1 - \big(\frac{V_v p_{vw}}{V_w p_{wv}}\big)\,\big]V_w| \ .\end{aligned} \tag{22}$$

Now we are in position to apply the estimates developed earlier. First, the visitation distribution V, appropriately weighted by conductances, gives the weighted visitation function U, which by Lemma 7.3.2 is a positive harmonic function for the process $\mathfrak{M}^b$. Given any $\tau > 0$, we may apply the Local Harnack Inequality and assume that mesh (P) is so small that

$$|1 - \frac{U(v)}{U(u)}| < \tau \ , \qquad |1 - \frac{U(v)}{U(w)}| < \tau \ .$$

By the identity $p_{vu}\mathcal{C}_v = p_{uv}\mathcal{C}_u$, we have

$$|1 - \big(\frac{V_v p_{vu}}{V_u p_{uv}}\big)| = |1 - \big(\frac{V_v \mathcal{C}_u}{V_u \mathcal{C}_v}\big)| = |1 - \frac{U(v)}{U(u)}| < \tau, \tag{23}$$

and likewise By the identity $p_{vu}\mathcal{C}_v = p_{uv}\mathcal{C}_u$, we have

$$|1 - \big(\frac{V_v p_{vu}}{V_w p_{vw}}\big)| < \tau \ . \tag{24}$$

The angle sum θ_u consists of the angle α plus angles from the other faces to which u belongs. By the Monotonicity Lemma, all these angles decrease when u increases, so we have $\big(\frac{\partial\theta_u}{\partial u}\big) < \big(\frac{\partial\alpha}{\partial u}\big) = g_1(u,v,w) < 0$. Along with Lemma 4.4.1(ii), this gives

$$|g_2(v,u,w)\big(\frac{\partial\theta_u}{\partial u}\big)^{-1}| < |\frac{g_2(v,u,w)}{g_1(u,v,w)}| \le C_1 \ ,$$

where C_1 is independent of P. Likewise,

$$|g_3(v,u,w)\big(\frac{\partial\theta_w}{\partial w}\big)^{-1}| < C_1 \ .$$

Putting this with (23) and (24) in (22) and noting that $\frac{dA}{dv}\frac{dv}{dt}$ is positive gives

$$\begin{aligned}|\frac{d\psi}{dt}| &\le C_1 \cdot \tau \cdot \big[\, |V_u| + |V_w| \,\big] + |\frac{dA}{dv}\frac{dv}{dt}| \\ &= C_1 \cdot \tau \cdot \big[\, |\big(\frac{\partial \theta_u}{\partial u}\big)\frac{du}{dt}| + |\big(\frac{\partial \theta_w}{\partial w}\big)\frac{dw}{dt}| \,\big] + \frac{dA}{dv}\frac{dv}{dt}\ .\end{aligned}$$

We are now in position to integrate. The term $|\frac{\partial \theta_u}{\partial u}| = -\frac{\partial \theta_u}{\partial u}$ goes to infinity as mesh (P) goes to zero, but we can apply Lemma 8.3.1 as follows: Write

$$\frac{\partial \theta_u}{\partial u} = \sum_{(u,y,z)} g_1(u,y,z)\ , \tag{25}$$

where the sum is over all triples (u,y,z) forming faces in the star of u. As t goes from 0 to 1, Lemma 8.3.1(i) implies that the s-radius u increases from its initial value $u_0 = u(0)$ to no more than $u_1 = u_0^{\mathfrak{C}_1}$. By Lemma 8.3.1(iii), when mesh (P) is small, we will have $u_1 < 4$, say. The inequality of Lemma 4.4.1(iii) now gives

$$\int_{u_0}^{u_1} |g_1(u,y,z)|\, du \le C_2 \int_{u_0}^{u_1} \frac{1}{\sqrt{u}(u-1)}\, du \le C_2 \int_{u_0}^{u_1} \frac{1}{u-1}\, du = C_2 \ln(\frac{u_0^{\mathfrak{C}_1}-1}{u_0-1})\ .$$

One easily verifies with L'Hôpital's rule that this is bounded by a constant C for u_0 small. Since there are at most $\mathfrak{d}$ faces in the sum (25), we see that for small mesh,

$$\int_0^1 |\frac{\partial \theta_u}{\partial u}(t)|\, dt < \mathfrak{d} \cdot C\ .$$

The same inequality holds for w.

In integrating $\frac{dA}{dv}\frac{dv}{dt}$, one must be cautious. The integral does not give the change in area of the face (v,u,w) between $t=0$ and $t=1$ (which is clearly small if mesh (P) is small) because we have been treating A as a function of v alone, keeping u and w constant. The fact that u and w change with t means that $\frac{dA}{dv}\frac{dv}{dt}$ is not the same as $\frac{dA}{dt}$. Nevertheless, we have more than enough estimates to handle this: By Lemma 4.4.3,

$$\int_0^1 \frac{dA}{dv}\frac{dv}{dt}\, dt \le C_4 \int_0^1 \frac{dv}{dt}\, dt = C_4(v(1) - v(0)),$$

where C_4 goes to zero as the s-radii v,u,w go to 1. By Lemma 8.3.1(iii), $v(0)$ and $v(1)$ are bounded by

$$\exp\{2\,\mathfrak{C}_3 \text{ mesh } (P)\}.$$

By making mesh (P) small, we can thus force

$$\int_0^1 \frac{dA}{dv}\frac{dv}{dt}\,dt < \tau\ .$$

In summary, by making mesh (P) small we have

$$|\psi(1)-\psi(0)| \le \int_0^1 |\frac{d\psi}{dt}|\,dt \le (2C_1C+1)\cdot\tau\ ,$$

for any preassigned $\tau > 0$. In particular, there is δ such that $|\psi(1)-\psi(0)| < \epsilon$ if mesh $(P) < \delta$. This completes our proof of Lemma 10.3.1. □

The Key Lemma follows from this result, so we have now established the convergence of the simplicial mappings to the conformal mapping in the Main Theorem. With that convergence confirmed, convergence of the ratio functions to the modulus of the derivative follows much as it does in the classical setting; see [14], where this is proven in quite general circumstance by means of the discrete Schwarz and Distortion theorems.

In the author's view, the identity contained in formulae (20) and (21) is central to the success of our program. To stengthen the intuition which lies behind it, we close the paper by revisiting the electrical circuit analogy suggested in Section 3.

11. Electrical Circuits

11.1. **Introduction.** The image of differential curvature moving among the circles of a packing in the same way that electrons move about an electrical circuit can be a very fruitful source of intuition, particularly since many of us share some insight into the behavior of electrical circuits without special knowledge of any underlying model. We introduced the electrical analogy in Section 3, and our intention here is to make the imagery more explicit by interpreting some of the details which have now emerged.

An electrical circuit or network consists of nodes and connecting wires. The circuit associated with a circle packing P has a node for each circle and a wire between nodes of tangent circles. In addition, a wire connects each node to ground, allowing for "leakage". Electrons represent (differential) quantities of angle, called curvature. The situation we face involves placing an initial curvature "charge" at specified boundary nodes, determining where it ultimately leaks to ground as it flows about the network, and drawing appropriate conclusions. Our discussion will be non-rigorous, and we take for granted the naive, discrete-time random walk model of electrical networks as described so well in Doyle and Snell [11], to which the reader is directed for further references.

11.2. **Circuits.** The overall electrical behavior of an electrical circuit N is determined by its combinatorics and by the electrical properties of the individual wires. The conductance of a wire, reciprocal of the more familiar electrical resistance, represents the ease with which current can move along the wire (without regard to direction); an electron moves from node to node based on transition probabilities, which in turn are

computed at each node (see (7)) from the conductances of the wires leaving that node. The movement of electricity through a wire is related by **Ohm's Law** to the voltage drop across the wire and the conductance. Consequently, by placing an initial charge on the network and observing the resulting currents, one can infer a voltage function on the nodes of N. **Kirchhoff's Law**, which states that the total current flowing into a node must equal the total current flowing out, implies that the voltage is given by a harmonic function.

An important special case for our purposes is that in which N has no connection to ground. A charge placed on the network cannot leave, and it is evident that it will distribute itself in such a way that no further net flow will take place. The ultimate distribution of the initial charge is proportional to what is termed the **stationary** distribution $\mathfrak{s}$. Suppose $\mathcal{C}_{ij}$ are the edge conductances of N, $\mathcal{C}_j$ the node conductances, and $\mathcal{C} = \sum_j \mathcal{C}_j$ the total conductance. The transition probabilities are defined by $p_{ij} = \mathcal{C}_{ij}/\mathcal{C}_i$ and comprise a transition matrix T. The stationary distribution $\mathfrak{s}$ is the unique probability distribution satisfying $\mathfrak{s} \cdot T = \mathfrak{s}$. One easily verifies that

$$\mathfrak{s} = [\mathfrak{s}_j] = [\mathcal{C}_1/\mathcal{C}, \mathcal{C}_2/\mathcal{C}, \cdots, \mathcal{C}_k/\mathcal{C}] \ .$$

Indeed, the lack of net flow across an edge i, j is expressed by

$$\mathfrak{s}_j p_{ij} = \frac{\mathcal{C}_{ij}}{\mathcal{C}} = \frac{\mathcal{C}_{ji}}{\mathcal{C}} = \mathfrak{s}_i p_{ji} \ . \tag{26}$$

Any distribution which is a constant multiple of $\mathfrak{s}$ is termed an **equilibrium** distribution. Note that such a distribution is in general nonconstant, although the fact that it is associated with no net current flow means that the corresponding voltage function is constant.

Now let us turn to a circuit N associated with some circle packing P. Our interest is in P with small mesh, and in this case N is large and the conductances to ground are small (Lemma 8.3.1(ii)). The work of Section 9 is directed at proving that such networks mimic (uniformly) those having no ground, as described above: Thus, though there is no equilibrium distribution *per se* (since the current dissipates) the quanta of curvature take many steps before leaking to ground; the visitation distribution V (§7.2.1) reflects their long term behavior and plays the role of an equilibrium distribution. The weighted distribution function U (§7.3.1) represents the voltage. Because the voltage is given by a harmonic function, we are able to use a Harnack inequality in order to quantify how close U comes to being constant. In essense, this measures how closely V mimics an equilibrium.

However, it is in Section 10 that the deeper connections among the circuit model, circle packing, and geometry emerge. After all, our real concern is not with current or voltage, but rather with the effects of the circuit behavior on a particular angle ψ of some face deep in the circle packing — that angle is associated with the ambient geometry. Even though our model of circuits is not completely appropriate for the task, we may draw further on the electrical analogy to suggest the relevance of geometry: Consider a thin (i.e., 2-dimensional) homogeneous plate Ω of conducting material. It

is perfectly reasonable to approximate its electrical properties by approximating its shape using a fine network of wires forming a circuit. Geometry enters with the word "homogeneous"; a static charge on Ω will, when it reaches equilibrium, have a spatial distribution which is nearly uniform deep within the plate's interior. However, when the plate is replaced by a discrete circuit, the charge will necessarily be concentrated at nodes. The discrete distribution of charge among the nodes which most closely approximates the continuous distribution of charge on the plate now depends heavily on the layout of the nodes; moreover, the wires must have appropriate conductances so that the charge actually assumes the desired distribution at equilibrium. All of this is easy if, for example, one could use an approximating circuit based on an infinite regular rectangular (or hexagonal) pattern of closely spaced wires. Notice that geometry enters very inconspicuously here, since symmetry alone suggests (rightly) that each wire should have the same conductance. But we don't have the luxury of choosing such nice networks; instead, we are faced with circuits coming from circle packings, and each has prescribed combinatorics and a geometric layout which is forced upon us by the radii of the circles. What should be the choice of edge conductances in this setting? Well, this is the very heart of our model: *The conductances determined by circle radii in accordance with Definition 6.5.1 seem to be the appropriate ones; they link the geometry of the pattern of circles to the equilibrium conditions of the corresponding electrical circuit.* We will close with a final computation showing this link, but first a comment on conductance: Unlike transition probabilities, conductances are properties of the "wires" themselves. The probabilities in Section 6 are motivated by conservation of hyperbolic angles/areas and have a convenient physical interpretation in terms of how much angle goes where; they depend on the whole ensemble of a flower, and typically $p_{ij} \neq p_{ji}$. The conductances, on the other hand, are more subtle; the conductance of an edge depends only on the radii of the circles at the two ends and their common neighbors and $\mathcal{C}_{ij} = \mathcal{C}_{ji}$. Though $\mathcal{C}_{ij}$ seems to have no direct physical meaning, it somehow represents the ease with which curvature flows (in either direction!) between nodes i and j.

11.3. **The Geometric/Electric Connection.** A final computation should confirm the intimacy of the link between the geometric and electrical behavior in our model: Suppose P is a circle packing laid out in the hyperbolic plane, and consider the particular face (v, u, w) represented in Figure 7. A is its area and ψ is the angle at v which has been of special interest. We use the various notations and auxiliary functions introduced earlier. Also, since our work is informal, we will be somewhat liberal with differential notation. For instance, we may reinterpret the visitation distribution V in terms of differential angle: Consider a node v_j. Each amount of curvature arriving at v_j must be passed along to area or to the neighbors; this is done by making an appropriate increase in radius dr_j resulting in a decrease in angle sum $d\theta_j$ which precisely matches the amount of curvature. We are justified, therefore, in writing

$$V = [d\theta_1, d\theta_2, \cdots, d\theta_k] \ .$$

(Recall that the initial curvature charge $d\lambda$ is negative, as are the differentials $d\theta_j$.)

The Circuit Computation: Recall that after placing a curvature charge on the boundary of the circuit and letting it flow to ground, V gives the quantity of curvature which has visited each of the various nodes (as distinct from the amount deposited as area at each node). When mesh is small, we have observed that V approximates an equilibrium distribution. For the sake of argument, *assume that leakage is zero and that V is an equilibrium distribution.* The identity (26) then implies

$$d\theta_i p_{ij} = d\theta_j p_{ji} \ . \tag{27}$$

Referring to Figure 7 and relying on associated s-radii and Definition 6.4.1, we have the following:

$$p_{vw} = -\,(\frac{\partial\omega}{\partial v})(\frac{\partial\theta_v}{\partial v})^{-1} \quad\Longrightarrow\quad d\theta_v p_{vw} = -\,(\frac{\partial\omega}{\partial v})\,dv \ ,$$

$$p_{wv} = -\,(\frac{\partial\gamma}{\partial w})(\frac{\partial\theta_w}{\partial w})^{-1} \quad\Longrightarrow\quad d\theta_w p_{wv} = -\,(\frac{\partial\gamma}{\partial w})\,dv \ .$$

Applying the identity (27),

$$dw = \frac{(\frac{\partial\omega}{\partial v})}{(\frac{\partial\gamma}{\partial w})}\,dv = \frac{h(w,a,u,v)}{h(v,a,u,w)}\,dv \ .$$

Likewise, $du = \dfrac{h(u,b,w,v)}{h(v,b,w,u)}\,dv$. These reflect the relationships in $d\mathbf{r}$ among radii adjustments upon reaching equilibrium — that is, knowing the total of adjustments made at v, one can compute the concomitant totals at u and w. Substituting these into the differential of the angle $d\psi = g_1(v,u,w)dv + g_2(v,u,w)du + g_3(v,u,w)dw$, we arrive at the following:

$$d\psi = [\, g_1(v,u,w) + g_2(v,u,w)\frac{h(w,a,u,v)}{h(v,a,u,w)} + g_3(v,u,w)\frac{h(w,a,u,v)}{h(v,a,u,w)}\,]\,dv \ . \tag{28}$$

The Geometric Conputation: Next we carry out a computation depending solely on the geometry of the circle packing P and independent of the dynamics of the circuit model; namely, we compute the differential of $A = \pi - g(v,u,w) - g(u,v,w) - g(w,u,v)$ as a function of the s-radius at v, giving

$$dA = -\,[g_1(v,u,w) + g_2(u,v,w) + g_3(w,u,v)]\,dv. \tag{29}$$

The Connection: If we substitute into (28) using the identities (1), note the order of the arguments, and compare to (29), we receive a most pleasant surprise! $d\psi = -\,dA$. That is:

The effect on the angle ψ when the radii are adjusted at all three of the circles v, u, w in accordance with the dictates of the electrical circuit model is precisely the negative of the effect on the area A when the radius is adjusted at v alone.

This, of course, is under the assumption that V is an equilibrium distribution. The formal epsilonics of Section 10 are needed to prove that $|d\psi + dA|$ indeed can be made arbitrarily small. Nonetheless, the equality $d\psi = -dA$ is true in spirit, and shows perhaps best of all how naturally and faithfully circle packing, hyperbolic geometry, and Markov processes fit together.

References

[1] Dov Aharonov, *The hexagonal packing lemma and discrete potential theory*, Canadian Math. Bulletin **33** (1990), 247–252.

[2] E. M. Andreev, *Convex polyhedra in Lobacevskii space*, Mat. Sbornik **81 (123)** (1970) (Russian).

[3] ———, *Convex polyhedra of finite volume in Lobacevskii space*, Mat. Sbornik **83** (1970), 256–260 (Russian).

[4] Alan F. Beardon, *The geometry of discrete groups*, GTM 91, Springer-Verlag, New York, Heidelberg, Berlin, 1983.

[5] Alan F. Beardon and Kenneth Stephenson, *The uniformization theorem for circle packings*, Indiana Univ. Math. J. **39** (1990), 1383–1425.

[6] ———, *The Schwarz-Pick lemma for circle packings*, Ill. J. Math. **35** (1991), 577–606.

[7] I. Benjamini and O. Schramm, *Harmonic functions on planar and almost planar graphs and manifolds, via circle packings*, preprint.

[8] Philip L. Bowers and Kenneth Stephenson, *Circle packings in surfaces of finite type: An in situ approach with application to moduli*, Topology **32** (1993), 157–183.

[9] Robert Brooks, *On the deformation theory of classical Schottky groups*, Duke Math. J. **52** (1985), 1009–1024.

[10] Yves Colin de Verdière, *Une principe variationnel pour les empilements de cercles*, Inventiones Mathematicae **104** (1991), 655–669.

[11] P. G. Doyle and J. L. Snell, *Random walks and electric networks*, Carus Math. Monographs, 22, Math Assoc. Amer., 1984.

[12] Tomasz Dubejko, *Infinite branched packings and discrete complex polynomials*, Jour. Lond. Math. Soc., to appear.

[13] ———, *Recurrent random walks, Liouville's theorem, and circle packings*, Proc. Camb. Phil. Soc., to appear.

[14] Tomasz Dubejko and Kenneth Stephenson, *The branched Schwarz lemma: a classical result via circle packing*, Mich. Math. J. **42** (1995), 211–234.

[15] ———, *Circle packing: Experiments in discrete analytic function theory*, Experimental Mathematics **4** (1995), no. 4, 307–348.

[16] Zheng-Xu He, *Solving Beltrami equations by circle packing*, Transactions Amer. Math. Soc. **322** (1990), 657–670.

[17] ———, *An estimate for hexagonal circle packings*, J. Differential Geometry **33** (1991), 395–412.

[18] Zheng-Xu He and Burt Rodin, *Convergence of circle packings of finite valence to Riemann mappings*, Comm. in Analysis and Geometry **1** (1993), 31–41.

[19] Zheng-Xu He and Oded Schramm, *Fixed points, Koebe uniformization and circle packings*, Ann. of Math. **137** (1993), 369–406.

[20] ———, *Hyperbolic and parabolic packings*, Discrete & Computational Geom. **14** (1995), 123–149.
[21] ———, *On the convergence of circle packings to the Riemann map*, Invent. Math. **125** (1996), 285–305.
[22] Koebe, *Kontaktprobleme der Konformen Abbildung*, Ber. Sächs. Akad. Wiss. Leipzig, Math.-Phys. Kl. **88** (1936), 141–164.
[23] O. Lehto and K. I. Virtanen, *Quasiconformal mappings in the plane*, 2nd ed., Springer-Verlag, New York, 1973.
[24] Gary L. Miller and William Thurston, *Separators in two and three dimensions*, Proceedings of the 22nd Annual ACM Symposium on Theory of Computing, ACM, Baltimore, May 1990, pp. 300–309.
[25] G. Pólya, *über eine Aufgabe der Wahrscheinlichkeitsrechnung betreffend die Irrfahrt im Strassennetz*, Math. Annalen **84** (1921), 149–160.
[26] Burt Rodin and Dennis Sullivan, *The convergence of circle packings to the Riemann mapping*, J. Differential Geometry **26** (1987), 349–360.
[27] Oded Schramm, *Rigidity of infinite (circle) packings*, Journal Amer. Math. Soc. **4** (1991), 127–149.
[28] Frank Spitzer, *Principles of random walk, graduate texts in math.*, vol. 34, Sringer-Verlag, New York, Heidelberg, Berlin, 1976.
[29] Kenneth Stephenson, *Circle packings in the approximation of conformal mappings*, Bulletin, Amer. Math. Soc. (Research Announcements) **23, no. 2** (1990), 407–415.
[30] William Thurston, *The geometry and topology of 3-manifolds*, Princeton University Notes, preprint.
[31] ———, *The finite Riemann mapping theorem*, 1985, Invited talk, An International Symposium at Purdue University on the occasion of the proof of the Bieberbach conjecture, March 1985.

University of Tennessee, Knoxville
E-mail address: kens@math.utk.edu